




# The Role of Thickening Agent Proportions in Optimizing Nanoemulsion Gel for Dermatophytosis Treatment

Xiao Zhang <sup>1,\*</sup>, Chen-Chen Wu<sup>1</sup>, Hua Jiang<sup>2</sup>, Jia-Fu Zhao <sup>1,3</sup>, Zhong-Jian Pan<sup>1</sup>, Yin Zheng <sup>1,3,\*</sup>

<sup>1</sup>College of Animal Science, Guizhou University, Guiyang, Guizhou, People's Republic of China; <sup>2</sup>College of Veterinary Medicine, Gansu Agriculture University, Lanzhou, Gansu, People's Republic of China; <sup>3</sup>Key Laboratory of Animal Genetics, Breeding and Reproduction in The Plateau Mountainous Region, Ministry of Education, Guizhou University, Guiyang, Guizhou, People's Republic of China

\*These authors contributed equally to this work

Correspondence: Yin Zheng, College of Animal Science, Guizhou University, Mingyi Building (Teaching and Research Center), Room 428, West Campus of Guizhou University, Huaxi District, Guiyang City, Guizhou Province, 550025, People's Republic of China, Email yzheng@gzu.edu.cn

**Background:** Adjusting thickening agent proportions in nanoemulsion gel (NG) balances its transdermal and topical delivery properties, making it more effective for dermatophytosis treatment.

**Methods:** Carbomer 940 and  $\alpha$ -pinene were used as model thickening agent and antifungal, respectively. A series of  $\alpha$ -pinene NGs ( $\alpha$ NG1,  $\alpha$ NG2,  $\alpha$ NG3) containing 0.5%, 0.75% and 1% (w/w) Carbomer 940 were developed and evaluated for stability, rheological properties, and skin irritation; assessed for ex vivo skin permeation, deposition, and fluorescent imaging of drug distribution within skin layers; and tested in vivo for efficacy against *Trichophyton rubrum* infection in guinea pigs, with PAS (Periodic Acid–Schiff) staining confirming fungal clearance.

**Results:** The steady-state skin flux rates of  $\alpha$ -pinene over 24 hours were  $\alpha$ NG1 ( $46.93 \pm 2.52 \mu\text{g}/\text{cm}^2/\text{h}$ ) >  $\alpha$ NG2 ( $26.01 \pm 2.65 \mu\text{g}/\text{cm}^2/\text{h}$ ) >  $\alpha$ NG3 ( $11.36 \pm 1.69 \mu\text{g}/\text{cm}^2/\text{h}$ ). The  $\alpha$ -pinene deposition in the epidermis/dermis for  $\alpha$ NG1 decreased substantially from 2 h ( $62.74 \pm 3.36 \mu\text{g}/\text{cm}^2$ ) to 12 h ( $11.7 \pm 2.24 \mu\text{g}/\text{cm}^2$ ). In contrast,  $\alpha$ NG2 showed relatively sustained deposition with 2 h ( $25.54 \pm 2.67 \mu\text{g}/\text{cm}^2$ ), 6 h ( $57.32 \pm 4.62 \mu\text{g}/\text{cm}^2$ ) and 12 h ( $23.69 \pm 3.29 \mu\text{g}/\text{cm}^2$ ).  $\alpha$ NG3 exhibited a slow increase from 2 h ( $18.32 \pm 2.11 \mu\text{g}/\text{cm}^2$ ) to 12 h ( $36.78 \pm 3.22 \mu\text{g}/\text{cm}^2$ ). The  $\alpha$ NG2 exhibited the highest efficacy and fungal clearance rates (71.42%, 79.17%), followed by  $\alpha$ NG1 (55.34% and 60.42%), and  $\alpha$ NG3 (43.21%, 52.08%). Fluorescent imaging confirmed  $\alpha$ NG2's higher drug deposition within the epidermis/dermis, while PAS staining showed a potent fungal clearance with  $\alpha$ NG2.

**Conclusion:** This study demonstrates that Carbomer 940 proportions significantly impact the transdermal performance of  $\alpha$ NG.  $\alpha$ NG2, with a moderate proportion, optimally enhances skin drug delivery and deposition, achieving superior therapeutic outcomes. These findings highlight the importance of optimizing thickening agent proportions to improve the efficacy of topical nanoemulsion gels.

**Keywords:** nanoemulsion gel, thickening agent proportions, drug delivery, dermatophytosis, alpha-pinene

## Introduction

Dermatophytes are the most common pathogenic fungi that cause tinea in humans and animals, affecting approximately 20–25% of the global population.<sup>1</sup> *Trichophyton rubrum* is responsible for about 80–90% of these infections.<sup>2,3</sup> The treatment of dermatophytosis is challenging due to rising antifungal resistance and the limited development of novel antifungal agents.<sup>1,4</sup> Dermatophyte infections typically localize in the stratum corneum (SC) and superficial epidermis but may also penetrate deeper structures such as the outer root sheath of hair follicles.<sup>1,3</sup> Conventional topical formulations, including emulsifiable pastes, gels, and tinctures, often struggle to deliver antifungal agents effectively through the formidable SC, limiting therapeutic outcomes.<sup>1,5</sup> These challenges emphasize the need for innovative formulation strategies to enhance drug delivery to infection sites, thereby improving therapeutic efficacy.

Nanoemulsion gel (NG) shows potential as an effective drug delivery system, particularly for transdermal applications.<sup>6–8</sup> These formulations incorporate nanoemulsion (NE) within a hydrogel matrix, which is primarily structured with thickening agents and water, effectively combining the solubility and bioavailability benefits of NE with the enhanced viscosity, adhesiveness, and biocompatibility provided by hydrogels.<sup>7,9</sup> This unique combination makes NG particularly effective for transdermal drug delivery, facilitating the permeation of drugs through the SC into deeper skin layers.<sup>6,7</sup> However, NG may encounter limitations, as excessive transdermal properties can lead to substantial drug delivery into systemic circulation, thereby reducing drug deposition in the epidermis and elevating the risk of adverse effects.<sup>9,10</sup> This issue is of particular concern when treating localized skin conditions like eczema, psoriasis, and tinea, where effective therapy relies on drug deposition in specific skin layers.<sup>11,12</sup> To address this, the role of thickening agents in the formulation of NG is pivotal, yet often underestimated. These agents, such as Carbomer 940, not only increase the viscosity of the gel but also modify the pore size of the mesh-like network within the gel matrix.<sup>9,12</sup> This structural alteration significantly influence the rate of drug release and skin permeation profiles, thereby affecting both the efficacy and safety of the therapy.<sup>13,14</sup> Consequently, by adjusting the thickening agent proportions, formulators can effectively tailor NGs to release drugs at a more intended rate.<sup>9,13</sup> It has been suggested that adjusting the proportions of thickening agents, such as Carbomer 940, within NG balances its transdermal and topical drug delivery properties. This optimization not only enhances control over drug release dynamics but also improves therapeutic outcomes for conditions like dermatophytosis, where localized drug deposition is crucial for efficacy, while minimizing systemic absorption and associated side effects.

In this study,  $\alpha$ -pinene and Carbomer 940 were selected as model antifungal agent and thickening agent, respectively, to investigate how thickening agent proportions within NG formulations influence therapeutic outcomes for dermatophytosis through topical application. Alpha-pinene, a monoterpene isolated from the leaves of *Platycladus orientalis* (L. Franco, which has demonstrated potent antifungal activity against *T. rubrum* through its ability to disrupt fungal cell membrane integrity and inhibit ergosterol synthesis.<sup>15</sup> Carbomer 940 was chosen for its widespread use in pharmaceutical formulations, well-established rheological properties, biocompatibility, and ability to modulate drug release profiles.<sup>12</sup> Here, we developed a series of  $\alpha$ -pinene nanoemulsion gels ( $\alpha$ NG1,  $\alpha$ NG2, and  $\alpha$ NG3) containing 0.5%, 0.75%, and 1% (w/w) Carbomer 940, respectively. Our objectives were to test stability, rheological properties, and skin irritation of  $\alpha$ NGs. Additionally, we evaluated their drug delivery performance through ex-vivo skin permeability tests, drug deposition analysis, and fluorescence imaging of drug distribution within skin layers, and assessed their therapeutic efficacy in a guinea pig model infected with *T. rubrum*, using Periodic Acid–Schiff (PAS) staining to confirm fungal clearance.

## Materials and Methods

### Chemical Compounds

Alpha-pinene (97% purity) was sourced from Beijing Bailingwei Technology Co., Ltd., Beijing, China. Terbinafine Hydrochloride Gel (TG), containing 1% (w/w) Terbinafine Hydrochloride, was provided by Sichuan Tiancheng Pharmaceuticals Co. Ltd., Mianyang, China. Carbomer 940 (>99% purity) and Periodic Acid–Schiff staining solution was obtained from Shanghai Yien Chemical Technology Co., Ltd., Shanghai, China. Polysorbates 20, 60, and 80 (>99% purity), as well as PPG-5-Ceteth-20 (PPG, >99% purity), were purchased from Tianjin Hengxing Reagent Factory, Tianjin, China. Coumarin-6 (98% purity) was procured from Shanghai Macklin Biochemical Technology Co., Ltd., Shanghai, China.

### Trichophyton rubrum Strain and Guinea Pigs

*Trichophyton rubrum* (ATCC 28188) was obtained from the American Type Culture Collection (Manassas, VA, USA).

Male guinea pigs (2 months old, weighing 300–500 g) were sourced from Chongqing Tengxin Biotechnology Co., Ltd. (Chongqing, China). All procedures performed in this study were approved by the Guizhou University Subcommittee of Experimental Animal Ethics (Approval No. EAE-GZU-2020-7015). All experiments were performed following Implementation Rules for the Administration of Laboratory Animals in Guizhou Province and Regulations for

the Administration of Affairs Concerning Experimental Animals of the People's Republic of China, ensuring the welfare of experimental animals.

## Development of $\alpha$ -Pinene Nanoemulsion

The methods here were applied from Azeem et al<sup>16</sup> with some modifications. Briefly, polysorbates 20, 60, 80, and PPG-5-Ceteth-20 (PPG) were tested as potential emulsifiers with  $\alpha$ -pinene, mixed in sequential ratios 1:1, 1:2, 1:3, 1:4, 1:5, 1:6, 1:7, 1:8 and 1:9 (w/w). Ultrapure water was added dropwise until the mixture became a clear, flowing liquid, defining the nanoemulsion region and aiding the construction of pseudo-ternary phase diagrams using Origin 9.0 software (OriginLab Corporation, Northampton, MA, USA). The emulsifier that resulted in the largest emulsification area was selected for subsequent use.

The  $\alpha$ -pinene nanoemulsions ( $\alpha$ NE1 through  $\alpha$ NE6) were formulated by mixing  $\alpha$ -pinene with the selected emulsifier in ratios 1:6, 1:6.5, 1:7, 1:7.5, 1:8 and 1:8.5 (w/w), respectively, using a water titration method to create a final system comprising 40 parts by weight. Each  $\alpha$ NE was first diluted tenfold with ultrapure water before characterization. Polydispersity index (PDI) and droplet size distribution (DSD) were determined using a Mastersizer 2000 particle size analyzer (Malvern Instruments, UK), and zeta potential measurements were performed using a Zetasizer Nano ZS (Malvern Instruments, UK). For transmission electron microscopy (TEM) observation, each sample dropped onto copper grids, air-dried, and observed under a JEOL JEM-1230 transmission electron microscope (JEOL Ltd., Tokyo, Japan) at 80 kV. The  $\alpha$ NE selected met the following criteria: a PDI below 0.2,<sup>17</sup> a DSD under 100 nm, and an absolute zeta potential of at least 10 mV.<sup>18</sup> TEM images further confirmed the absence of non-film forming emulsifiers and verified the uniform morphology of the nanoemulsion droplets. Among the formulations meeting these criteria, the one with the smallest DSD was chosen for further studies.

## Preparation of $\alpha$ -Pinene Nanoemulsion Gels

A series of  $\alpha$ -pinene nanoemulsion gels ( $\alpha$ NGs) were prepared by incorporating the selected  $\alpha$ NE into gel bases containing Carbomer 940, as described by Hussain et al.<sup>19</sup> Briefly, Carbomer 940 was uniformly dispersed in deionized water and stirred at 120 rpm at room temperature for 3 hours to prepare gel bases with 1%, 1.5%, and 2% (w/w) concentrations. Triethanolamine was then added dropwise to these gel bases, stirring at 60 rpm for 3 hours to adjust the pH to 6.9 $\pm$ 0.1, using a pH meter (Shanghai Yidian Scientific Instrument Co., Ltd., Shanghai, China). The gel bases were left to rest overnight to ensure adequate crosslinking of Carbomer 940. The following day, the selected  $\alpha$ NE was incorporated into these gel bases at a 1:1 (w/w) ratio, stirring continuously (60 rpm) for 3 hours to produce  $\alpha$ NG1,  $\alpha$ NG2, and  $\alpha$ NG3, which contained 0.5%, 0.75%, and 1% Carbomer 940 (w/w), respectively.

## Characterization of $\alpha$ -Pinene Nanoemulsion Gels

The formulations  $\alpha$ NG1,  $\alpha$ NG2, and  $\alpha$ NG3 were analyzed to assess their physicochemical properties and nanostructural characteristics.<sup>9</sup> The pH of each formulation was measured as previously described during gel base preparation. For measurements of DSD, PDI, zeta potential and nanostructural observations via TEM, the samples were diluted tenfold with deionized water, filtered through Whatman #1 filter paper, and the resulting filtrates were analyzed following the procedures outlined in the "Development of  $\alpha$ -pinene nanoemulsion" section. The viscosity of undiluted samples was measured using a viscometer (Middleboro, MA, USA) with spindle No. 62 operated at 25 rpm and 25°C. Spreadability was evaluated by placing 500 mg sample on a glass plate (10 cm $\times$ 7 cm), marking a 2 cm circle in diameter, covering it with a 20 g glass plate (1 mm thick), and adding an additional 500 g glass plate. The diameter of the spread sample was measured after 5 min. Gel strength was determined by placing a 110 g steel ball onto the gel sample and recording the time required for the ball to sink 5 cm. All measurements were performed in triplicate.

## Stability Tests of $\alpha$ -Pinene Nanoemulsion Gels

The stability of formulations  $\alpha$ NG1,  $\alpha$ NG2, and  $\alpha$ NG3 was evaluated by subjecting the samples to stress conditions: either heating in a water bath at 50°C for 30 min or centrifugation at 12,000 rpm for 30 min. After these stress tests, the samples were analyzed for changes in DSD, PDI, zeta potential, viscosity, spreadability, and gel strength, as described in

the “Characterization of  $\alpha$ -pinene nanoemulsion gels” section. Additionally, these parameters were reassessed after storage for 60, and 180 days to detect any changes over time. All measurements were performed in triplicate.

## Skin Irritation Tests

Skin irritation tests were adapted from Draize et al.<sup>20</sup> Thirty guinea pigs were randomly divided into five groups: three test groups ( $\alpha$ NG1,  $\alpha$ NG2,  $\alpha$ NG3), a negative control (treated with PBS), and a positive control (treated with 10% formalin). Each guinea pig was depilated on two 3 cm  $\times$  3 cm dorsal areas. One area was left intact, while the other was abraded using 120-grit sandpaper (STARCKE<sup>®</sup>, Melle, Germany) to gently disrupt the SC without causing bleeding. Treatments were applied to designated areas, covered with gauze for six hours, and observed at 24, 48, and 72 h post-application. The erythema and edema intensity were scored according to the Draize test scale as follows:<sup>20</sup> 0, no observable erythema or edema; 1, very slight erythema or edema (barely perceptible); 2, well-defined erythema or slight edema; 3, moderate-to-severe erythema or moderate edema; 4, severe erythema (beet-red) or severe edema (extending beyond the area of exposure).

The average scores were classified as follows: 0–0.49, no irritation; 0.5–2.99, mild irritation; 3.0–5.99, moderate irritation; 6–8, severe irritation.

## Determination of $\alpha$ -Pinene in $\alpha$ -Pinene Nanoemulsion Gels

To analyze the concentration of  $\alpha$ -pinene in  $\alpha$ NGs,  $\alpha$ NG2 was selected as the representative sample, and Blank Nanoemulsion Gel (BNG,  $\alpha$ NG3 without  $\alpha$ -pinene) served as the control. The analysis was conducted using an HPLC method developed with the Agilent 1260 Series system (Agilent Technologies Inc., California, USA), equipped with an Extend-C18 column (250 mm  $\times$  4.6 mm, 5  $\mu$ m particle size). The column temperature was maintained at 40°C, using a mobile phase of acetonitrile and water in a 4:1 (v/v) ratio at a flow rate of 1 mL/min, with detection at a wavelength of 254 nm. For sample preparation, both  $\alpha$ NG2 and BNG were diluted tenfold with acetonitrile, sonicated to remove dissolved gases, and filtered through a 0.45  $\mu$ m membrane filter before injection into the HPLC system. Calibration curves were constructed using standard  $\alpha$ -pinene solutions, ensuring linearity over the tested concentration range. The developed method was validated for linearity, precision, accuracy, and recovery rate to ensure the reliability and reproducibility of the analytical results.

## Ex Vivo Skin Permeability Tests

Ex vivo skin permeability tests were conducted using a transdermal diffusion system (Shanghai Huanghai Pharmaceutical Inspection Instrument Co., Ltd., Shanghai, China).<sup>21</sup> Skin samples were obtained from four male guinea pigs, each assigned to one of four treatment groups:  $\alpha$ NG1,  $\alpha$ NG2,  $\alpha$ NG3, and conventional  $\alpha$ -pinene gel ( $\alpha$ CG, containing 0.75% Carbomer 940). Following depilation and a 24-hour rest period, a 2 cm diameter section of abdominal skin was excised from each guinea pig and mounted in a Franz diffusion cell. The dermis was positioned towards the receiver chamber containing 5 mL phosphate-buffered saline (PBS) with 1% (w/v) polysorbate 80, while the SC faced the donor chamber with a diffusion area of 0.785 cm<sup>2</sup>. For each treatment, 4 g of the respective formulation was applied to the donor chamber. The system was maintained at 37.0  $\pm$  0.1°C, with a magnetic stirrer operating at 350 rpm at the bottom of the receiver chamber to ensure uniform mixing. Samples (2 mL) were withdrawn from the receiver chamber at intervals of 0.5, 1, 2, 3, 4, 6, 8, 12, 16, and 24 hours, immediately replenished with equal volume of pre-warmed PBS containing 1% (w/v) polysorbate 80. The  $\alpha$ -pinene concentrations in these samples were quantified using high-performance liquid chromatography (HPLC). The cumulative amount of  $\alpha$ -pinene permeated per unit area ( $Q_n$ ,  $\mu$ g/cm<sup>2</sup>) was plotted against time to generate permeation curves. The steady-state skin flux ( $J_{ss}$ ,  $\mu$ g/cm<sup>2</sup>/h) was derived from the linear portion of the permeation curve between 0.5 and 24 hours. The enhancement ratio was determined by comparing the  $J_{ss}$  values of the  $\alpha$ NGs with that of  $\alpha$ CG. The experiments were performed in triplicate.

## Alpha-Pinene Deposition in the Stratum Corneum and Epidermis/Dermis

Following procedures and treatments similar to those in the ex vivo skin permeability test,  $\alpha$ -pinene concentrations in the SC and epidermis/dermis were measured at 2, 6, and 12 hours.<sup>22</sup> At each time point, skin samples were collected from

one guinea pig per treatment group:  $\alpha$ NG1,  $\alpha$ NG2,  $\alpha$ NG3, and  $\alpha$ CG. The skin samples were washed with warm PBS, dried, and processed. The SC was removed by tape-stripping, and the remaining epidermis/dermis layers were collected. Each layer was extracted separately with 4 mL of methanol at 20°C for 1 hour with intermittent vortexing. After extraction, the samples were centrifuged at 3000 rpm for 10 min. The resulting supernatants were analyzed using HPLC to quantify  $\alpha$ -pinene concentrations, which were expressed as “ $\mu\text{g}/\text{cm}^2$ ” to reflect the amount in each skin layer. The experiments were performed in triplicate.

## Fluorescent Imaging of Drug Distribution Within Skin

Coumarin-6 was dissolved in  $\alpha$ -pinene to prepare the oil phase.<sup>23</sup> The formulations, including  $\alpha$ NGs ( $\alpha$ NG1,  $\alpha$ NG2 and  $\alpha$ NG3) and  $\alpha$ CG, were then prepared as previously described. Twelve male guinea pigs were randomly assigned to four treatment groups ( $\alpha$ NG1,  $\alpha$ NG2,  $\alpha$ NG3, and  $\alpha$ CG), with three guinea pigs per group. Following depilation and 24 h rest period, 0.5 g of assigned formulation was applied to the abdominal skin of each guinea pig, which was then covered with occlusive chambers. At 2, 6, and 12 h post-treatment, one guinea pig from each treatment group, and the skin sample was prepared as described in ex vivo skin permeability tests, immediately frozen, and sectioned. The frozen sections were subsequently observed using laser scanning confocal microscopy (LSCM) at an excitation wavelength of 466 nm.

## A Guinea Pig Model Infected With *Trichophyton rubrum*

A guinea pig model infected with *Trichophyton rubrum* was established and verified.<sup>24</sup> Specifically, *T. rubrum* was subcultured on Sabouraud dextrose agar (SDA) plates at 28°C for 7 days. Spores were harvested by washing the colonies with Sabouraud dextrose broth (SDB) and filtering, then diluted to  $1.5 \times 10^6$  CFU/mL. Prior to inoculation, guinea pigs received daily intramuscular injections of triamcinolone acetonide acetate (1 mL/kg; Zhejiang Xianju Pharmaceutic Co. Ltd., Xianju, China) for three consecutive days to suppress immune responses. For inoculation, the guinea pigs were anesthetized with ether, and the hair on a 3 cm $\times$ 3 cm abdominal area was removed using an electric clipper and a disposable razor, followed by abrasion with sterile sandpaper. Then, 100  $\mu\text{L}$  of the *T. rubrum* spore suspension was applied to the abraded skin, which was covered with sterile gauze for three consecutive days. Upon removal of the gauze, the inoculated area was inspected for signs of dermatophytosis. Shed skin flakes from the area were cultured on SDA plates at 28°C and 65% humidity for seven days to verify *T. rubrum* growth. Hair samples from the infected site were treated with 10% potassium hydroxide (KOH) and examined under a microscope to confirm the presence of fungal hyphae.

## Therapeutic Efficacy Test

Guinea pigs were divided into six groups of 5 animals each, totalling 30 guinea pigs.<sup>25</sup> The groups consisted of three  $\alpha$ NG treatment groups ( $\alpha$ NG1,  $\alpha$ NG2, and  $\alpha$ NG3), a positive drug control group using Terbinafine Hydrochloride Gel (TG) containing 1% w/w Terbinafine Hydrochloride (Sichuan Tiancheng Pharmaceuticals Co. Ltd., Mianyang, China), an untreated infected group (positive control), and an untreated healthy group (negative control). Except for the negative control group, all other groups underwent the *Trichophyton rubrum* infection model establishment process as described earlier. For the negative control group, guinea pigs did not receive fungal inoculation but underwent similar procedures to simulate mechanical stress, including hair removal with an electric clipper and a disposable razor, followed by abrasion with sterile sandpaper.

Upon confirmation of infection on day 4 post-inoculation, the therapeutic efficacy test was initiated. The infected skin areas of guinea pigs in each treatment group received daily topical applications of 0.5 g of the assigned formulation ( $\alpha$ NG1,  $\alpha$ NG2,  $\alpha$ NG3 or TG) for ten consecutive days. Lesion severity was assessed daily for 14 days using a standardized scoring system ranging from 0 to 5.26 where: 0, no visible lesions or signs of infection; 1, very mild lesions with slight redness and no hair loss; 2, mild lesions with noticeable redness and minimal hair loss; 3, moderate lesions with pronounced redness, swelling, and partial hair loss; 4, severe lesions with extensive hair loss, significant redness and swelling; 5, very severe lesions with nearly complete or complete hair loss over a large skin area and possibly accompanied by crusting and scaling. The average daily lesion scores for each group were used to plot lesion severity curves over time, illustrating the progression or regression of the infection.

The therapeutic effectiveness was evaluated using two parameters: efficacy rate and fungal clearance rate, recorded on days 6 and 14 post-treatment.<sup>26</sup> The efficacy rates were calculated using the following formula:

$$\text{Efficacy rate (\%)} = 100 - \frac{\text{Total score of lesion scoring for each group} \times 100}{\text{Total score of lesion scoring for the untreated positive control}} \quad (1)$$

For fungal clearance rate assessment, one hair from each of the four quadrants of the infected lesion area was collected from all five guinea pigs in each group. These hairs were cultured on Sabouraud dextrose agar (SDA) and incubated for 5 days at 28°C and 65% humidity. Fungal clearance rates were determined using the following formula:

$$\text{Fungal clearance rate (\%)} = 100 - \left( \frac{\text{Number of fungal hyphae penetrating hair for each group} \times 100}{\text{Number for the untreated positive control}} \right) \quad (2)$$

## Histopathological Examination

Periodic acid-Schiff (PAS) staining was utilized to visualize fungal structures and tissue morphology.<sup>27</sup> At the end of therapeutic efficacy test, one guinea pig from each group was selected for histopathological examination. Specifically, for the  $\alpha$ NG1,  $\alpha$ NG2,  $\alpha$ NG3, and TG groups, guinea pigs with a lesion score of 0 were chosen. For the positive control, the guinea pig with the lowest lesion score was selected. For the negative control, any guinea pig was suitable. These selected guinea pigs were anesthetized, and skin samples were excised from the infected areas (for  $\alpha$ NG1,  $\alpha$ NG2,  $\alpha$ NG3, TG and positive control groups) or a corresponding region (for the negative control) using the corneal trephine. The samples were fixed in 10% formalin solution for 24 hours, dehydrated with ethanol, embedded in paraffin, and sectioned. These sections were stained with PAS and examined under a light microscope.

## Statistical Analysis

Data were expressed as mean  $\pm$  standard deviation, but the Draize test, enhanced ratio values, efficacy rates and fungal clearance rates are in their original form. One-way analysis of variance (ANOVA) was used to compare values across groups. Statistical significance was determined using the Tukey-Kramer multiple comparison test. The chi-square test was used to analyze the efficacy rates and fungal clearance rates across groups. Differences were considered statistically significant at  $P < 0.05$  and highly significant at  $P < 0.01$ .

## Results

### Development of $\alpha$ -Pinene Nanoemulsion

In the pseudo-ternary phase diagrams (Figure 1), Tween 80 exhibited the largest emulsification region. Utilizing the water titration method,  $\alpha$ -pinene and Polysorbate 80 at mass ratios of 1:6 to 1:8.5, with increments of 0.5, resulted in the formation of optically clear  $\alpha$ NEs ( $\alpha$ NE1 to  $\alpha$ NE6). TEM images (Figure 2) showed that droplet sizes within nanoscale range ( $<100$  nm) across all formulations, with some non-film forming emulsifier visible in  $\alpha$ NE4,  $\alpha$ NE5, and  $\alpha$ NE6 (Figure 2D-F, a); both the DSD and PDI (Figure 3) exhibited a decreasing trend from  $\alpha$ NE1 to  $\alpha$ NE6, and zeta potentials (Figure 4) became more negative as Polysorbate 80 concentration increased. Among the formulations, both  $\alpha$ NE2 and  $\alpha$ NE3 met the predetermined criteria, but  $\alpha$ NE3 exhibited a smaller DSD compared to  $\alpha$ NE2. Thus,  $\alpha$ NE3 was selected for the preparation of  $\alpha$ NGs, with  $\alpha$ -Pinene, Polysorbate 80, and water at a mass ratio of 1:7:32.

### Characterization and Stability Tests of $\alpha$ -Pinene Nanoemulsion Gels

The  $\alpha$ NGs exhibited a clear and transparent appearance. The pH values of  $\alpha$ NG1,  $\alpha$ NG2, and  $\alpha$ NG3 were  $6.8 \pm 0.1$ ,  $6.9 \pm 0.1$ , and  $6.9 \pm 0.1$ , respectively. Transmission electron microscopy images (Figure 5) demonstrate that all  $\alpha$ NGs maintain nanoscale particle sizes, along with the presence of some non-film forming emulsifiers (Figure 5A-C, a), resulting in a uniform particle size distribution. The DSD, PDI, and zeta potential values of  $\alpha$ NGs are documented in Table 1. Specifically, the DSD values for all  $\alpha$ NGs exceeded 100 nm, significantly larger than those of  $\alpha$ NE3 ( $P < 0.01$ ), with  $\alpha$ NG3 showing the largest DSD followed by  $\alpha$ NG2 and  $\alpha$ NG1. The zeta potentials of  $\alpha$ NGs were less negative than those of  $\alpha$ NE3 ( $P < 0.01$ ), while PDIs showed no significant changes in comparison to  $\alpha$ NE3 ( $P > 0.05$ ). At day 0, the

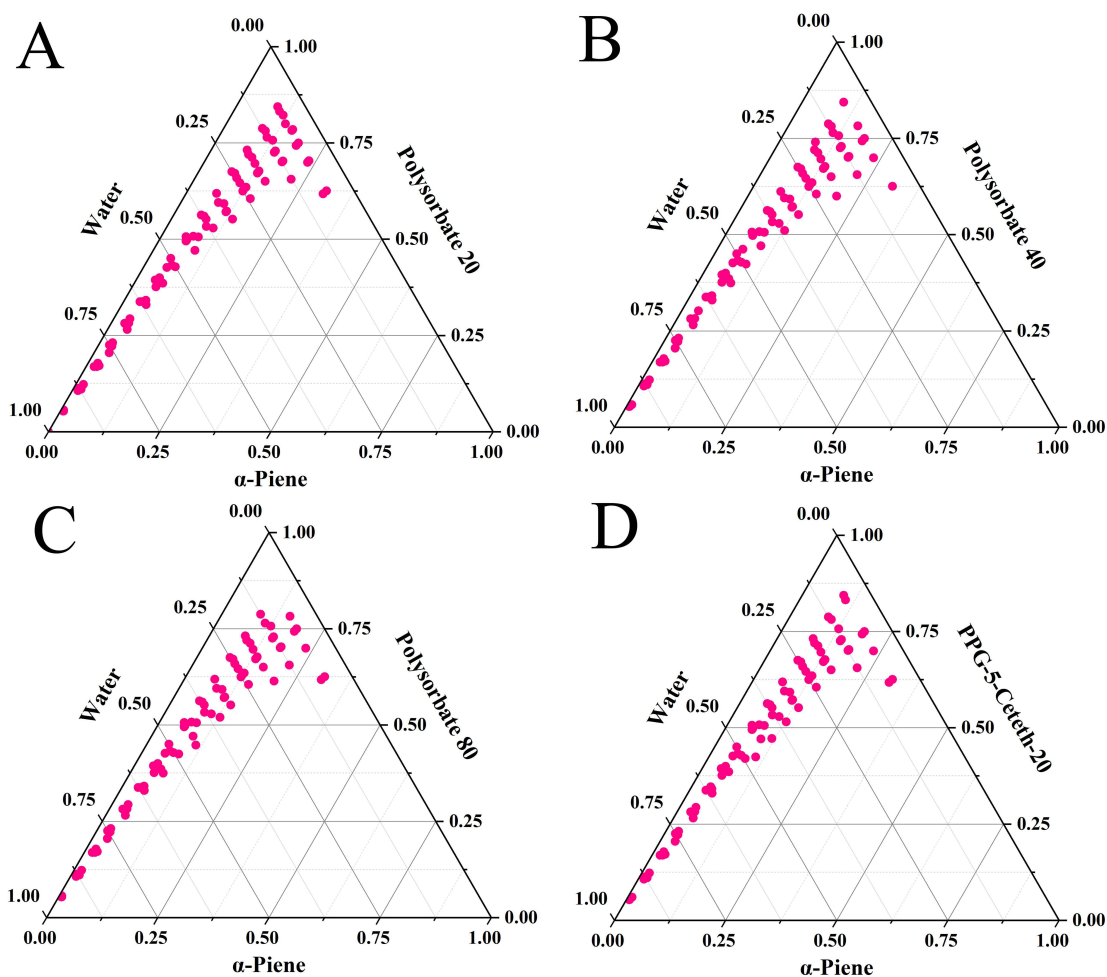


**Figure 1** The ternary-pseudo diagrams of four emulsifiers combined with  $\alpha$ -pinene.  
**Notes:** (A) Polysorbate 20; (B) Polysorbate 40; (C) Polysorbate 80; (D) PPG-5-Ceteth-20.

viscosities of  $\alpha$ NG1,  $\alpha$ NG2, and  $\alpha$ NG3 were  $1329 \pm 0.5$  cps,  $1340 \pm 0.6$  cps and  $1389 \pm 0.8$  cps, respectively. Spreadability measurements showed  $\alpha$ NG1 with the highest value ( $7.6 \pm 0.3$  cm), followed by  $\alpha$ NG2 ( $7.0 \pm 0.4$  cm) and  $\alpha$ NG3 ( $6.3 \pm 0.2$  cm). Gel strength increased progressively from  $\alpha$ NG1 ( $48.3 \pm 1.0$  s) to  $\alpha$ NG2 ( $59.8 \pm 1.3$  s) and  $\alpha$ NG3 ( $67.4 \pm 0.9$  s).

Stability tests under extreme conditions, including heating and centrifugation, showed no significant changes in DSD, PDI, zeta potential viscosity, spreadability or gel strength compared to their untreated forms ( $P > 0.05$ , data not shown). Similarly,  $\alpha$ NGs remained stable over 60 and 180 days of storage, with no notable variations in these parameters ( $P > 0.05$ , data not shown).

## Skin Irritation Tests

The results of the skin irritation test were shown in Table 2. Throughout the experiment, neither PBS (negative control) nor  $\alpha$ NGs induced skin irritation on intact or abraded skin; conversely, a 10% formalin solution caused strong skin irritation during the test, scoring 8 points.

## Determination of $\alpha$ -Pinene in $\alpha$ -Pinene Nanoemulsion Gels

Chromatographic analysis of the  $\alpha$ NG or BNG identified well-defined peaks for  $\alpha$ -pinene, with no interference from excipients, as illustrated in Figure 6. Calibration curves for  $\alpha$ -pinene spanned concentrations from 0.5325 to 132.5  $\mu$ g/mL, resulting in a regression equation of  $y=1591.2x + 8149.3$  with a correlation coefficient ( $r^2$ ) of 0.9938. Precision of

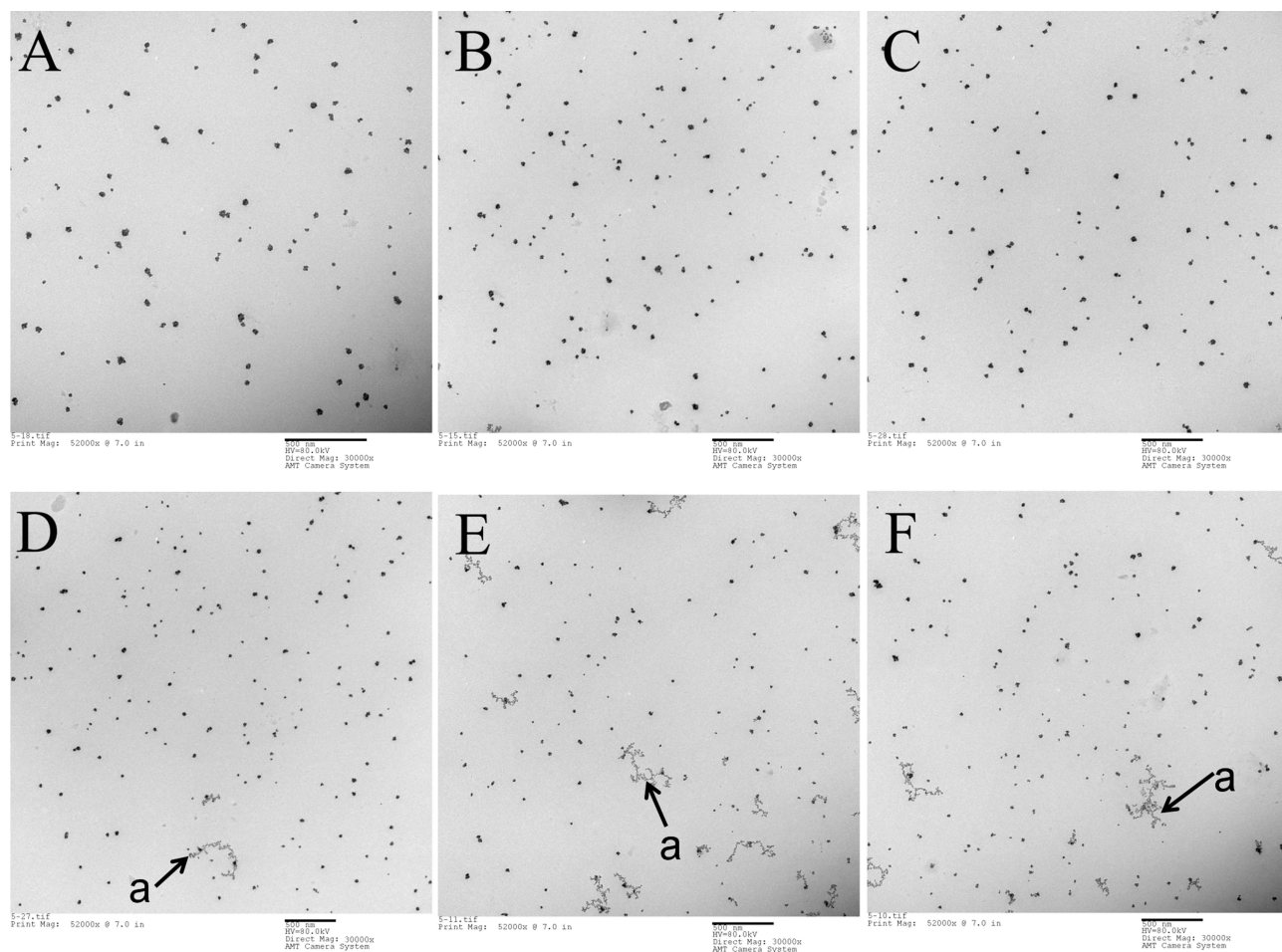


**Figure 2** TEM images of  $\alpha$ -pinene nanoemulsions prepared with Polysorbate 80 at various mass ratios.

**Notes:** (A)  $\alpha$ NE1; (B)  $\alpha$ NE2; (C)  $\alpha$ NE3; (D)  $\alpha$ NE4; (E)  $\alpha$ NE5; (F)  $\alpha$ NE6.  $\alpha$ NE1,  $\alpha$ NE2,  $\alpha$ NE3,  $\alpha$ NE4,  $\alpha$ NE5 and  $\alpha$ NE6:  $\alpha$ -pinene nanoemulsion where mass ratios of  $\alpha$ -pinene /Polysorbate were 1:6, 1:6.5, 1:7, 1:7.5, 1:8 and 1:8.5. "a" indicates the non-film forming emulsifier.

**Abbreviation:**  $\alpha$ NE,  $\alpha$ -pinene Nanoemulsion.

the method was indicated by standard deviations of less than 2% for both intraday and interday assays. The recovery rate of  $\alpha$ -pinene was  $99.45\% \pm 0.23\%$ .

## Ex Vivo Skin Permeability Tests

The  $Q_n$  and  $J_{ss}$  values for  $\alpha$ -pinene from  $\alpha$ NGs and  $\alpha$ CG were presented in Table 3 and Figure 7. The  $Q_n$  values increased in the order of  $\alpha$ CG <  $\alpha$ NG3 <  $\alpha$ NG2 <  $\alpha$ NG1, with highly significant differences between the groups ( $P < 0.01$ ). Similarly, the  $J_{ss}$  values followed the same trend:  $\alpha$ NG1 >  $\alpha$ NG2 >  $\alpha$ NG3 >  $\alpha$ CG. Compared to  $\alpha$ CG, the  $J_{ss}$  values for  $\alpha$ NG1,  $\alpha$ NG2,  $\alpha$ NG3 were 10.29-, 5.70- and 2.49-fold higher, respectively. The  $J_{ss}$  values of  $\alpha$ NG2 and  $\alpha$ NG3 were significantly less than that of  $\alpha$ NG1 ( $P < 0.01$ ).

## Alpha-Pinene Deposition in the Stratum Corneum and Epidermis/Dermis

The  $\alpha$ -pinene deposition amount in the SC and epidermis/dermis at 2 h, 6 h and 12 h were shown in Table 4. In the SC, at 2 h,  $\alpha$ NG1 exhibited the largest deposition followed by  $\alpha$ NG2 and  $\alpha$ NG3 ( $P < 0.05$  or 0.01); however, at 6 h and 12 h,  $\alpha$ NG3 exhibited a larger accumulation followed by  $\alpha$ NG2 and  $\alpha$ NG1 ( $P < 0.05$  or 0.01); meanwhile,  $\alpha$ CG achieved significantly larger  $\alpha$ -pinene deposition only at 12 h compared to  $\alpha$ NGs ( $P < 0.01$ ). For the epidermis/dermis, at 2 h the  $\alpha$ -pinene deposition was in the order of  $\alpha$ NG1 >  $\alpha$ NG2 >  $\alpha$ NG3 ( $P < 0.05$  or 0.01); however, at 6 h,  $\alpha$ NG2 exhibited the largest deposition followed by  $\alpha$ NG3 and  $\alpha$ NG1 ( $P < 0.01$ ); and at 12 h,  $\alpha$ NG3 exhibited a larger deposition followed by



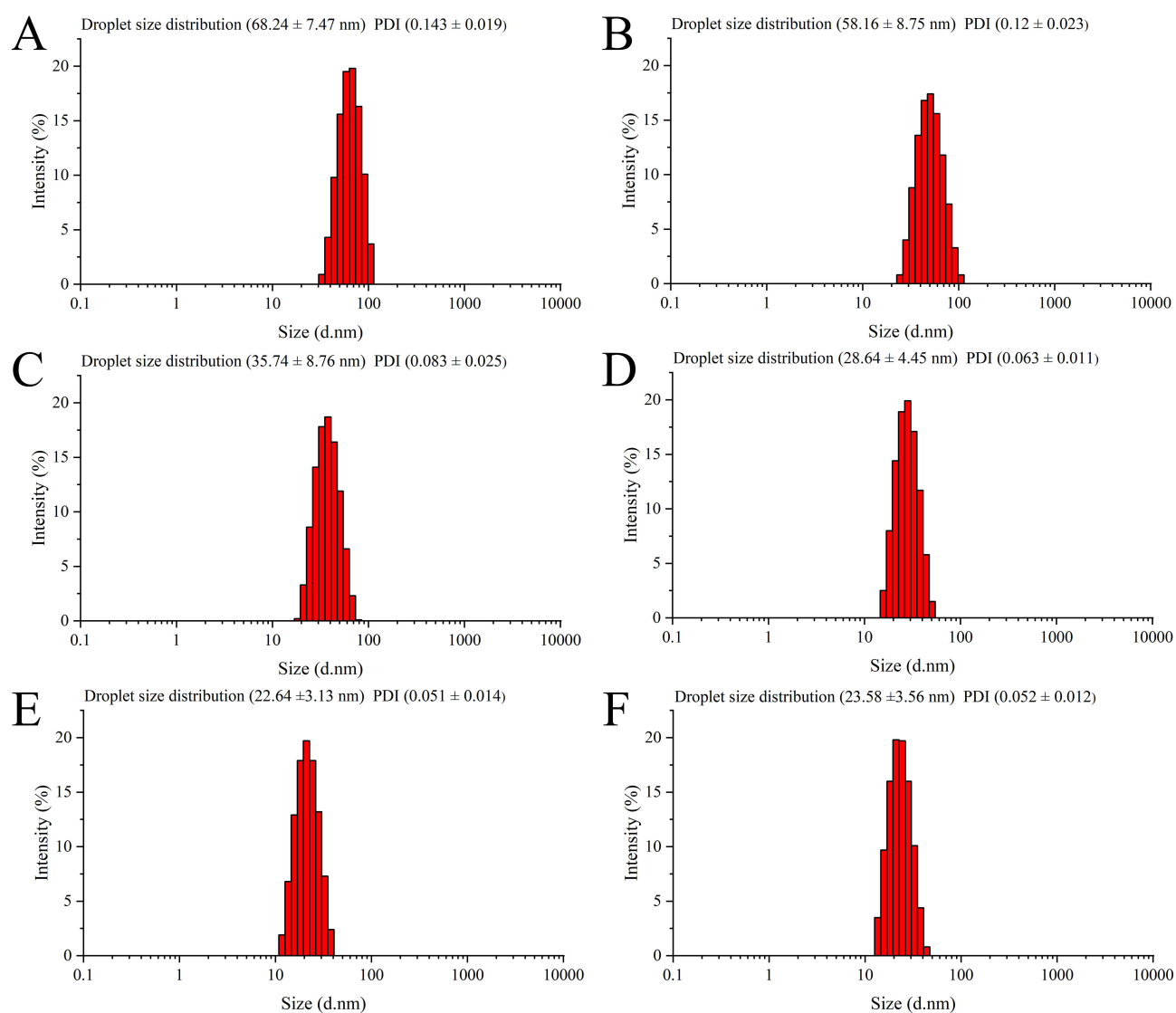


**Figure 3** Droplet size distribution/PDI values of  $\alpha$ -pinene nanoemulsions using Polysorbate 80 at different mass ratios.

**Notes:** (A)  $\alpha$ NE1; (B)  $\alpha$ NE2; (C)  $\alpha$ NE3; (D)  $\alpha$ NE4; (E)  $\alpha$ NE5; (F)  $\alpha$ NE6.  $\alpha$ NE1,  $\alpha$ NE2,  $\alpha$ NE3,  $\alpha$ NE4,  $\alpha$ NE5 and  $\alpha$ NE6:  $\alpha$ -pinene nanoemulsion where mass ratios of  $\alpha$ -pinene /Polysorbate were 1:6, 1:6.5, 1:7, 1:7.5, 1:8 and 1:8.5.

**Abbreviation:**  $\alpha$ NE,  $\alpha$ -pinene Nanoemulsion.

$\alpha$ NG2 and  $\alpha$ NG1 ( $P < 0.01$ ); additionally,  $\alpha$ CG steadily increased deposition during the test and only exhibited larger deposition only at 12 h compared to  $\alpha$ NGs ( $P < 0.01$ ).

## Fluorescent Imaging of Drug Distribution Within Skin

The fluorescence distribution of  $\alpha$ -pinene at 2 h, 6 h, and 12 h post-treatment with  $\alpha$ NGs and  $\alpha$ CG was illustrated in Figure 8. At 2 h, fluorescence from  $\alpha$ NG1 was observed primarily in the SC and epidermis/dermis (Figure 8A). By 6 h and 12 h, the fluorescence intensity decreased, with minimal signals remaining in the SC and epidermis (Figure 8B-C). For  $\alpha$ NG2, fluorescence was initially localized within the SC at 2 h (Figure 8D), extended into the epidermis/dermis at 6 h and persisted in both layers at 12 h (Figure 8E-F). In contrast,  $\alpha$ NG3 exhibited weak fluorescence at 2 h, which increased significantly at 6h, spreading to both layers by 12 h (Figure 8G-I). For  $\alpha$ CG, fluorescence remained largely within the SC throughout the test period, with limited signals observed in the epidermis at 12 h (Figure 8J-L). Bright fluorescent bands were observed within the SC for  $\alpha$ NG2 at 2 h and 6 h (arrow “a” in Figure 8D-E), while for  $\alpha$ NG3 and  $\alpha$ CG, these bands became more prominent at 6 h and 12 h (arrow “a” in Figure 8H and I, K and L).

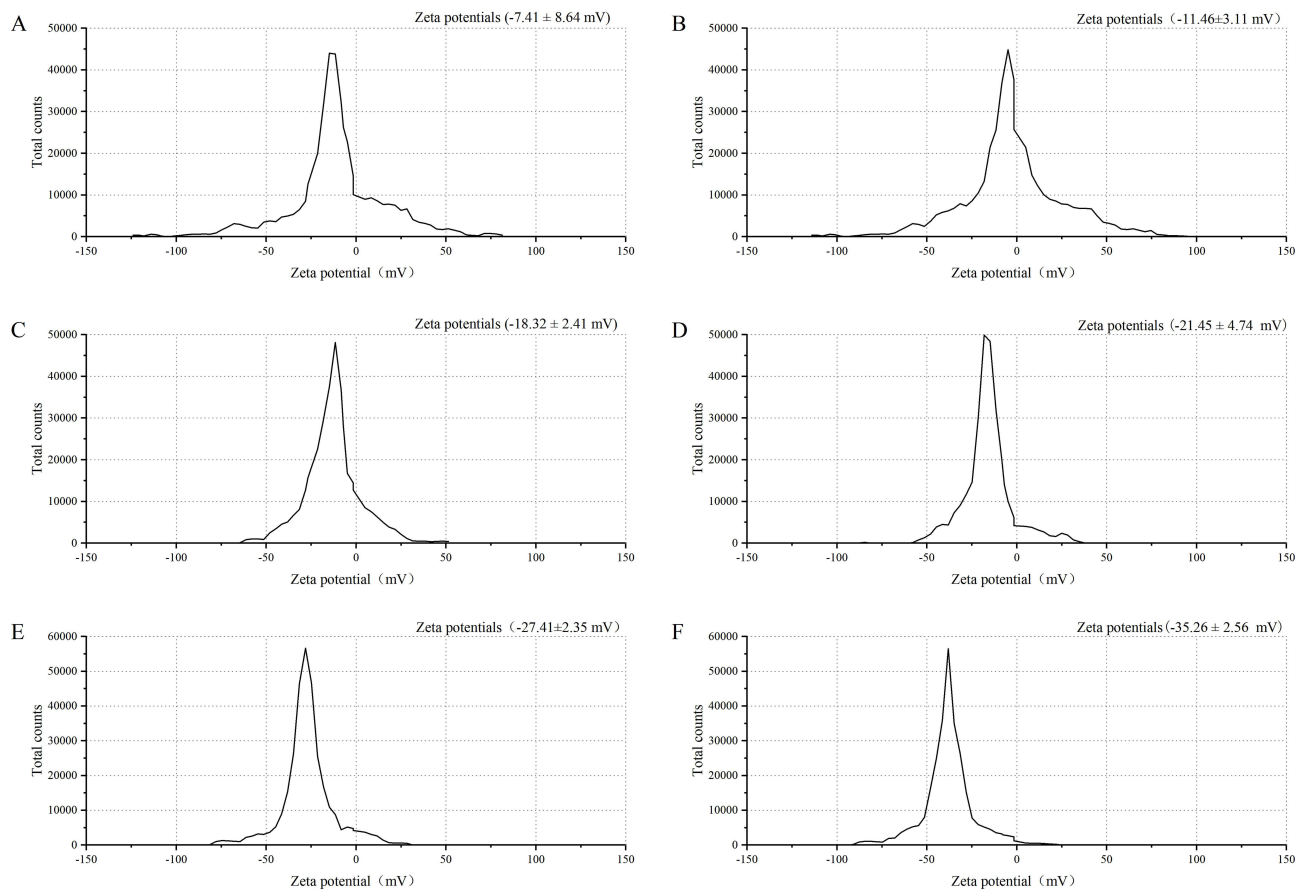


**Figure 4** Zeta potential values of  $\alpha$ -pinene nanoemulsions using Polysorbate 80 at different mass ratios.

**Notes:** (A)  $\alpha$ NE1; (B)  $\alpha$ NE2; (C)  $\alpha$ NE3; (D)  $\alpha$ NE4; (E)  $\alpha$ NE5; (F)  $\alpha$ NE6.  $\alpha$ NE1,  $\alpha$ NE2,  $\alpha$ NE3,  $\alpha$ NE4,  $\alpha$ NE5 and  $\alpha$ NE6:  $\alpha$ -pinene nanoemulsion where mass ratios of  $\alpha$ -pinene/Polysorbate were 1:6, 1:6.5, 1:7, 1:7.5, 1:8 and 1:8.5.

**Abbreviations:**  $\alpha$ NE,  $\alpha$ -pinene Nanoemulsion.

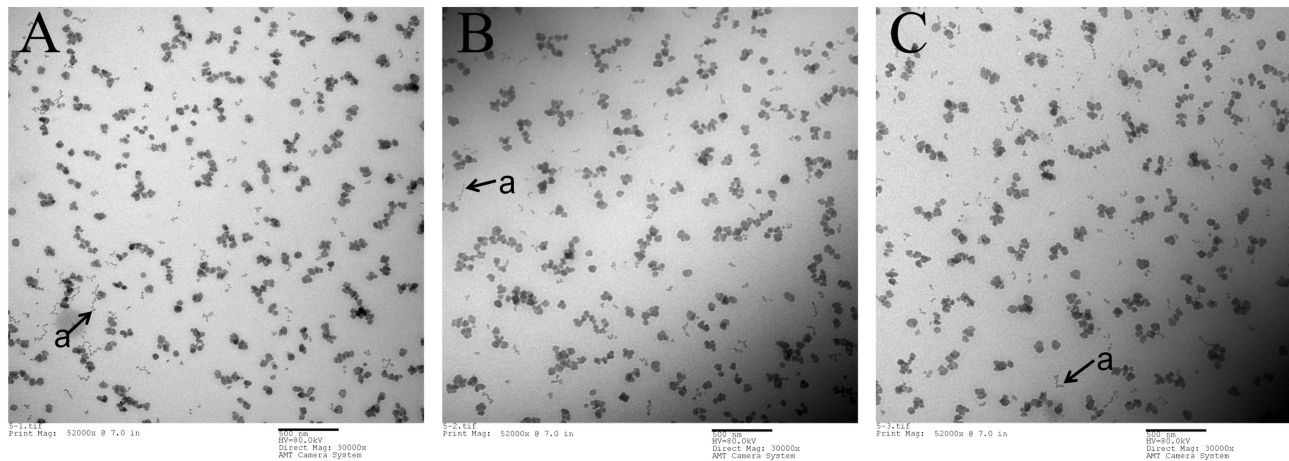


**Figure 5** TEM images of  $\alpha$ NGs.

**Notes:** (A)  $\alpha$ NG1; (B)  $\alpha$ NG2; (C)  $\alpha$ NG.  $\alpha$ NG1,  $\alpha$ NG2 and  $\alpha$ NG3:  $\alpha$ NE3 containing 0.5, 0.75%, and 1% (w/w) Carbomer 940. The arrow labeled "a" indicates excess polysorbate 80, which led to the formation of non-film-forming structures.

**Abbreviations:**  $\alpha$ NE,  $\alpha$ -pinene Nanoemulsion;  $\alpha$ NG,  $\alpha$ NE gel.

**Table 1** The DSD, PDI and Zeta Potential of  $\alpha$ NE3 and  $\alpha$ NGs

Formulations	DSD (nm)	PDI	Zeta potential (mv)
$\alpha$ NE3	35.74±8.76 <sup>cC</sup>	0.083±0.025 <sup>a</sup>	-18.32±2.41 <sup>aA</sup>
$\alpha$ NG1	105.89±10.52 <sup>bA</sup>	0.089±0.027 <sup>a</sup>	-7.64±3.23 <sup>bB</sup>
$\alpha$ NG2	116.33±9.17 <sup>abA</sup>	0.078±0.019 <sup>a</sup>	-9.65±2.18 <sup>bB</sup>
$\alpha$ NG3	134.23±12.59 <sup>aA</sup>	0.082±0.021 <sup>a</sup>	-8.17±1.52 <sup>bB</sup>

**Notes:**  $\alpha$ NG1,  $\alpha$ NG2,  $\alpha$ NG3:  $\alpha$ NE gels containing 0.5, 0.75%, and 1% (w/w) Carbomer 940, respectively. Within the same column, different lowercase letters indicate significant differences ( $P < 0.05$ ), and different uppercase letters indicate highly significant differences ( $P < 0.01$ ).

**Abbreviations:**  $\alpha$ NE,  $\alpha$ -piene Nanoemulsion;  $\alpha$ NG,  $\alpha$ -piene Nanoemulsion gel; DSD, droplet size distribution; PDI, polydispersity index.

**Table 2** The Mean Scores of Skin Erythema and Edema in Each Group After 24 h, 48 h and 72 h of Drug Treatment

Formulations	Intact Skin Erythema/Swollen Scores (n=6)			Abraded Skin Erythema/Swollen scores (n=6)		
	24 h	48 h	72 h	24 h	48 h	72 h
$\alpha$ NG1	0	0	0	0	0	0
$\alpha$ NG2	0	0	0	0	0	0
$\alpha$ NG3	0	0	0	0	0	0
PBS	0	0	0	0	0	0
10%formalin	6.5	8	8	8	8	8

**Notes:**  $\alpha$ NG1,  $\alpha$ NG2,  $\alpha$ NG3:  $\alpha$ NE gels containing 0.5, 0.75%, and 1% (w/w) Carbomer 940, respectively.

**Abbreviations:**  $\alpha$ NG,  $\alpha$ -Piene Nanoemulsion gel; PBS, Phosphate Buffered Saline.

## Guinea Pig Model Infected With *Trichophyton rubrum*

The results concerning Guinea pig model infected with *T. rubrum* were shown in Figure 9. On the third day post-inoculation with *T. rubrum*, alopecia, scabs, white scales and severe erythema were observed at the infection site (Figure 9A). Subsequently, the shed skin flakes and hairs of the infected site were cultured on SDA plates for 7 days. Hyphal penetration through the hair shafts was observed under the microscope (arrow “a” in Figure 9B), and typical *T. rubrum* colonies and red pigment production were observed (Figure 9C-D).

## Therapeutic Efficacy Test

The therapeutic efficacy of  $\alpha$ NGs on dermatophytosis was depicted in Table 5 and Figures 10 and 11.

On the first day post-treatment, guinea pigs in the positive control and other treatment groups exhibited noticeable symptoms of dermatophytosis at the infected skin area, such as erythema and scales (Figure 10B-F). From day 1 to day 5 post-treatment, all  $\alpha$ NGs led to a notable reduction in lesion scores, with  $\alpha$ NG1 demonstrating the greatest reduction in lesion severity (Figure 11). From day 6 to day 14 post-treatment,  $\alpha$ NG2 exhibited a greater reduction in lesion scores compared to  $\alpha$ NG1 and  $\alpha$ NG3 (Figure 11).

At 6 days post-treatment, the efficacy and fungal clearance rates of  $\alpha$ NG1 were significantly higher than those of  $\alpha$ NG2 and  $\alpha$ NG3 ( $P < 0.01$  or  $0.05$ ); notably, its efficacy rates were higher than those of the positive drug control TG ( $P < 0.05$ ). At 14 days post-treatment,  $\alpha$ NG2 achieved the highest efficacy and fungal clearance rates among  $\alpha$ NGs ( $P < 0.01$ ), although still lower than those of TG ( $P < 0.05$  or  $0.01$ ). At the end of the test, the skin at the infected site in each treatment group appeared visually healed, although partial hair regrowth was observed (Figure 10I-L).

## Histopathological Examination

PAS staining was conducted on the infected skin areas of guinea pigs randomly selected from each group after the therapeutic efficacy test, and the results are presented in Figure 12.

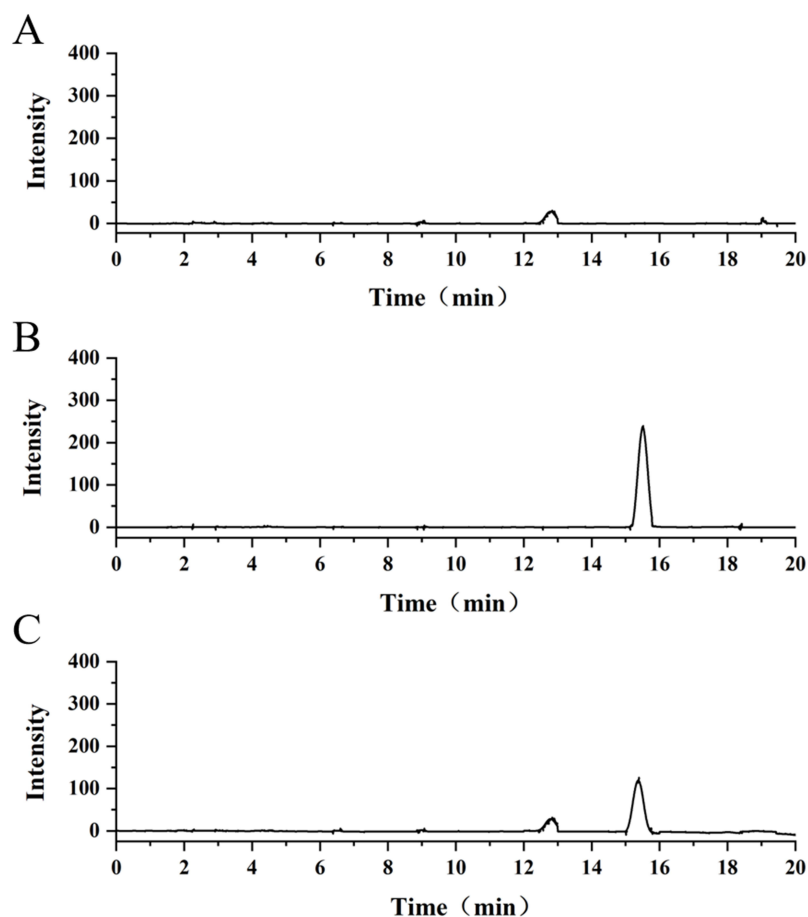


**Figure 6** HPLC diagrams of different formulations.

**Notes:** (A) BNG; (B) standard  $\alpha$ -pinene; (C)  $\alpha$ NG2.  $\alpha$ NG2:  $\alpha$ NE3 containing 0.75% (w/w) Carbomer 940.

**Abbreviations:**  $\alpha$ NG,  $\alpha$ -pinene Nanoemulsion gel; BNG, blank Nanoemulsion gel.

In the negative control group, the SC, epidermis and dermis appeared intact, with numerous healthy hair follicles, hair shafts, and sebaceous glands clearly visible (arrows a-e in Figure 12A). In contrast, the positive control group exhibited a significantly thickened SC with evidence of shedding, and hyphae and spores were observed in the outer root sheath and inner root sheath of hair follicles (arrow f in Figure 12B). Among  $\alpha$ NG treatment groups, the SC of  $\alpha$ NG1-treated skin was severely disrupted or removed (arrow h in Figure 12C). While for  $\alpha$ NG2 and  $\alpha$ NG3, the SC remained relatively

**Table 3** Ex Vivo Skin Permeation Parameters of  $\alpha$ -Pinene Over 24 h

Formulations	$Q_n$ ( $\mu\text{g}/\text{cm}^2$ )	$J_{ss}$ ( $\mu\text{g}/\text{cm}^2/\text{h}$ )	ER
$\alpha$ NG1	$1126.37 \pm 54.33^{\text{aA}}$	$46.93 \pm 2.52^{\text{aA}}$	10.29
$\alpha$ NG2	$624.182 \pm 31.44^{\text{bB}}$	$26.01 \pm 2.65^{\text{bB}}$	5.70
$\alpha$ NG3	$272.737 \pm 25.34^{\text{cC}}$	$11.36 \pm 1.69^{\text{cC}}$	2.49
$\alpha$ CG	$109.451 \pm 28.11^{\text{dD}}$	$4.56 \pm 2.23^{\text{dD}}$	1

**Notes:**  $\alpha$ NG1,  $\alpha$ NG2,  $\alpha$ NG3:  $\alpha$ NE gels containing 0.5, 0.75%, and 1% (w/w) Carbomer 940, respectively;  $\alpha$ CG, conventional gel containing  $\alpha$ -pinene; Within the same column, different lowercase letters indicate significant differences ( $P < 0.05$ ), and different uppercase letters indicate highly significant differences ( $P < 0.01$ ).

**Abbreviations:**  $\alpha$ NG,  $\alpha$ -pinene Nanoemulsion gel;  $\alpha$ CG,  $\alpha$ -pinene Conventional gel;  $Q_n$ , Cumulative  $\alpha$ -pinene amounts per unit area;  $J_{ss}$ , the steady-state skin flux; ER, Enhanced Ratio, was determined by comparing the  $J_{ss}$  values of the  $\alpha$ NGs with that of  $\alpha$ CG.

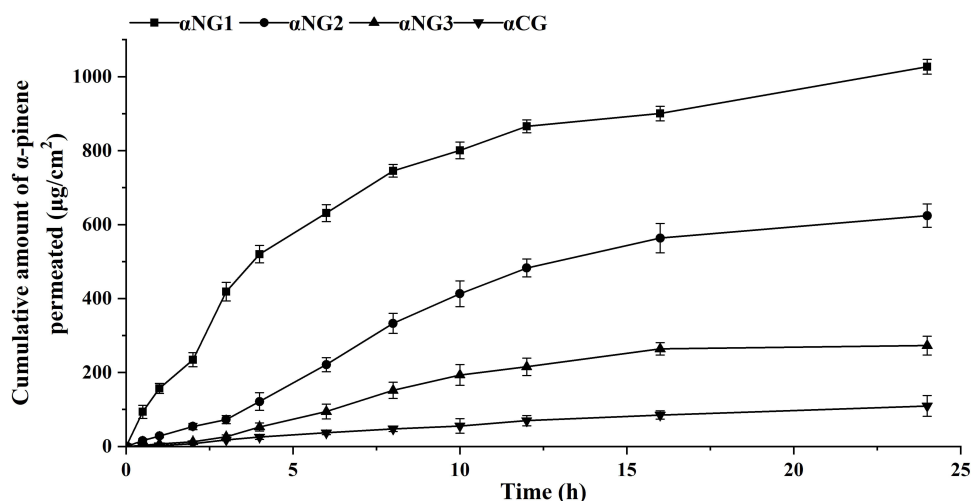


**Figure 7** Cumulative permeation of  $\alpha$ -pinene through Guinea pig skin abdominal in vitro.

**Notes:**  $\alpha$ NG1,  $\alpha$ NG2,  $\alpha$ NG3:  $\alpha$ NE3 containing 0.5, 0.75%, and 1% (w/w) Carbomer 940;  $\alpha$ CG, conventional gel containing  $\alpha$ -pinene.

**Abbreviations:**  $\alpha$ NG,  $\alpha$ -pinene Nanoemulsion gel;  $\alpha$ CG,  $\alpha$ -pinene Conventional gel.

intact (arrow i in Figure 12D and E). Notably,  $\alpha$ NG2 showed minimal spore-infected hair follicles, closely resembling the results observed for TG treatment group (arrow f and g in Figure 12F). However, spore presence and mycelium growth were still evident in the hair follicles of  $\alpha$ NG1 and  $\alpha$ NG3 treatment groups (arrows g in Figure 12C and f in E).

## Discussion

NG is recognized for its transdermal delivery potential,<sup>6,7,10</sup> however, its application in dermatophytosis treatment necessitates a formulation strategy that ensures enhanced local drug deposition while minimizing systemic absorption.<sup>9,11,12</sup> Our findings highlight the critical importance of Carbomer 940 proportions, demonstrating specific levels significantly improve drug retention at infection sites. By balancing NG's transdermal and topical drug delivery properties, the optimized NG address the challenge of maintaining effective local drug concentrations while avoiding excessive systemic uptake. The following sections explore the broader implications of these findings for advancing NG in dermatophytosis treatment.

In our evaluation of different emulsifiers, polysorbate 80 was determined to be the most effective for emulsifying  $\alpha$ -pinene in nanoemulsion formulations, as demonstrated by pseudo-phase diagrams (Figure 1). The careful adjustment of the ratios of polysorbate 80 to  $\alpha$ -pinene proved critical in achieving the most stable and effective emulsion properties. Higher ratios of polysorbate 80 resulted in smaller droplet sizes, which corresponded with increased absolute zeta potentials. This increase in absolute zeta potential is attributed to the smaller nanoemulsion droplets having an increased surface-to-volume ratio, which allows for a higher density of surface OH<sup>-</sup> groups.<sup>28,29</sup> This indicates a more stabilized nanoemulsion system. Notably, our studies also showed that an excess of polysorbate 80

**Table 4** The Amount of  $\alpha$ -Pinene Deposition in Certain Skin Layers at 2 h, 6 h and 12 h

Model Drug	Formulations	Stratum Corneum			Epidermis/dermis		
		2 h	6 h	12 h	2 h	6 h	12 h
$\alpha$ -pinene ( $\mu\text{g}/\text{cm}^2$ )	$\alpha$ NG1	9.83±0.49 <sup>aA</sup>	9.73±1.03 <sup>CB</sup>	2.65±0.84 <sup>dD</sup>	62.74±3.36 <sup>aA</sup>	27.08±2.43 <sup>bBC</sup>	11.7±2.24 <sup>dD</sup>
	$\alpha$ NG2	5.13±0.82 <sup>bAB</sup>	11.31±0.99 <sup>bAB</sup>	5.19±0.75 <sup>cC</sup>	25.54±2.67 <sup>bB</sup>	57.32±4.62 <sup>aA</sup>	23.69±3.29 <sup>cC</sup>
	$\alpha$ NG3	3.96±0.66 <sup>cB</sup>	13.65±1.54 <sup>aA</sup>	9.81±0.71 <sup>bB</sup>	13.47±1.14 <sup>cC</sup>	30.83±2.29 <sup>bB</sup>	32.99±2.89 <sup>bB</sup>
	$\alpha$ CG	1.48±0.22 <sup>dC</sup>	5.63±0.87 <sup>dC</sup>	12.14±0.96 <sup>aA</sup>	6.58±0.72 <sup>dC</sup>	23.34±2.45 <sup>cC</sup>	45.04±3.73 <sup>aA</sup>

**Notes:**  $\alpha$ NG1,  $\alpha$ NG2,  $\alpha$ NG3:  $\alpha$ NE3 containing 0.5, 0.75%, and 1% (w/w) Carbomer 940;  $\alpha$ CG, conventional gel containing  $\alpha$ -pinene; Within the same column, different lowercase letters indicate significant differences ( $P < 0.05$ ), and different uppercase letters indicate highly significant differences ( $P < 0.01$ ).

**Abbreviations:**  $\alpha$ NG,  $\alpha$ -pinene Nanoemulsion gel;  $\alpha$ CG,  $\alpha$ -pinene Conventional gel.

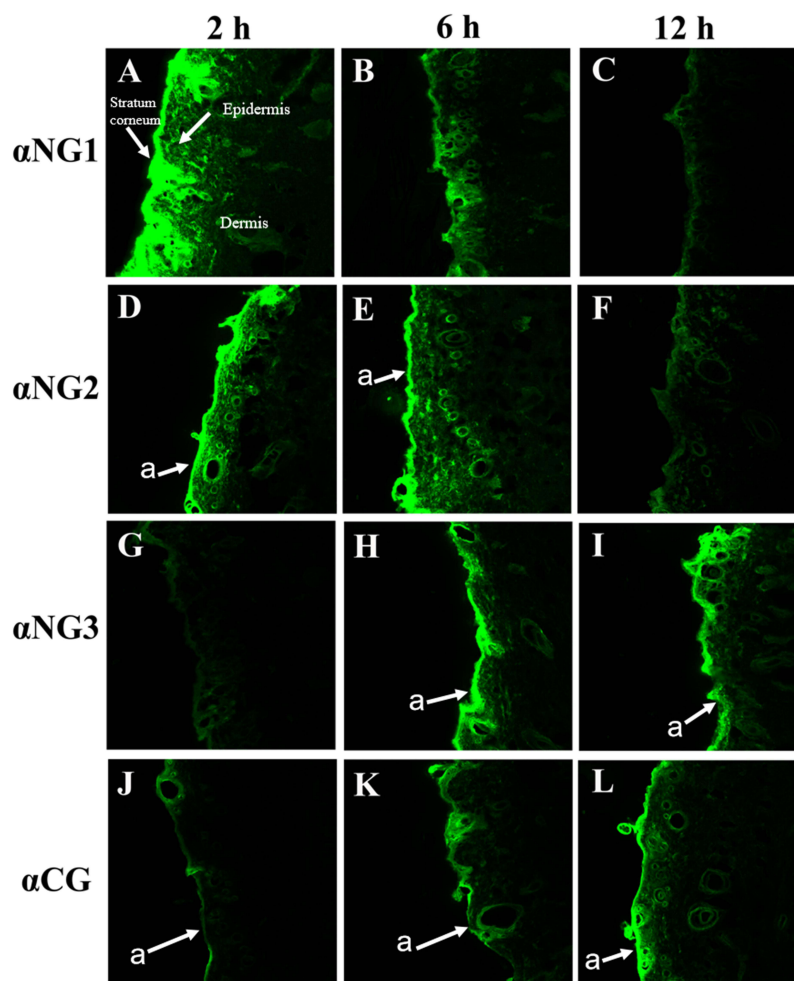


**Figure 8** Fluorescent images of drug distribution in the abdominal skin of Guinea pigs 2, 6, and 12 h post-treatment.

**Notes:**  $\alpha$ NG1,  $\alpha$ NG2,  $\alpha$ NG3:  $\alpha$ NE3 containing 0.5, 0.75%, and 1% (w/w) Carbomer 940;  $\alpha$ CG, conventional gel containing  $\alpha$ -pinene. (A-C) The trace of drugs in skin layers with  $\alpha$ NG1, (D-F)  $\alpha$ NG2, (G-I)  $\alpha$ NG3, and (J-L)  $\alpha$ CG at time intervals 2, 6 and 12 h, respectively. “a” is the bright band formed by drug deposition at the stratum corneum.  
**Abbreviations:**  $\alpha$ NG,  $\alpha$ -piene Nanoemulsion gel;  $\alpha$ CG,  $\alpha$ -piene conventional gel.

led to the formation of non-film-forming structures, as evident in specific micrographs (Figure 2D-F, a), indicating that the emulsifiers were not fully utilized, potentially compromising drug release uniformity and nanoemulsion consistency.<sup>30,31</sup> Consequently,  $\alpha$ NE3 was selected for  $\alpha$ NG preparation due to its absence of non-film-forming structures (Figure 2C), relatively smaller droplet sizes (Figure 3C), and favorable zeta potential (Figure 4C). These attributes ensure stability during storage and promote uniform dispersion into the gel matrix,<sup>32</sup> providing a solid foundation for the  $\alpha$ NG development.

The  $\alpha$ NGs were formulated with a neutral pH range of 6.8–7.0, compatible with the skin’s natural pH and suitable for topical application. Incorporating  $\alpha$ NE3 into a gel matrix containing various concentrations of Carbomer 940 resulted in larger droplet sizes, as shown by TEM images (Figure 3), while maintaining comparable PDI values. This was mainly due to suboptimal absolute zeta potential values (<30 mv), which were insufficient to fully prevent particle aggregation during blending.<sup>18,29</sup>

Stability tests (data not shown) demonstrated that the gel matrix effectively restricted droplet movement, minimizing aggregation and enhancing nanoemulsion stability, consistent with other reports.<sup>9,33</sup> Additionally, the Draize test results confirmed the non-irritating nature of  $\alpha$ NGs, supporting their safety for topical application. This aspect is crucial for patient compliance and the success of a dermatological treatments.<sup>7,11</sup>

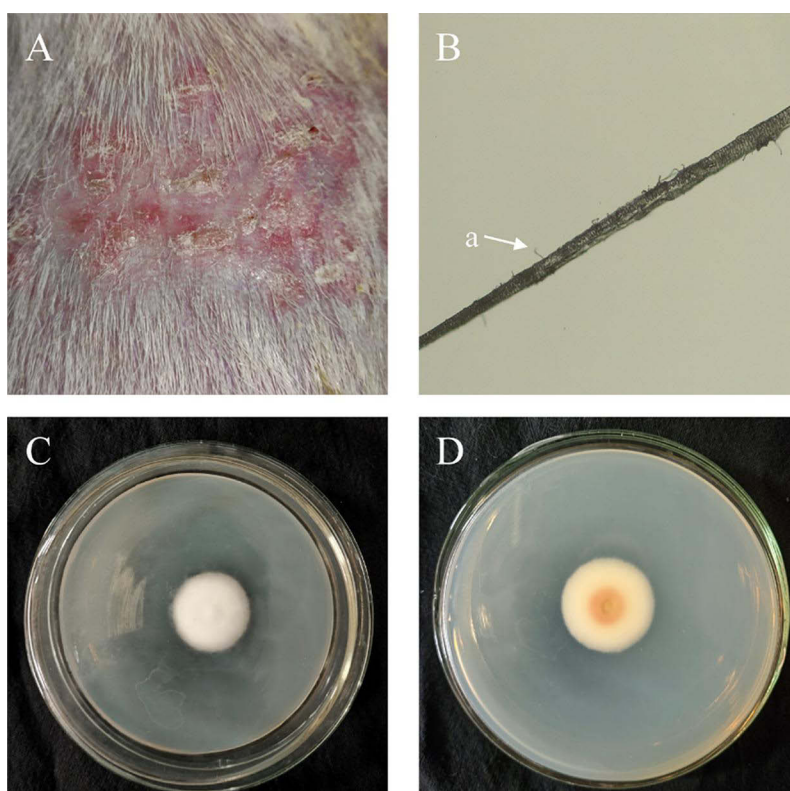


**Figure 9** Validation of Guinea pig model infected with *Trichophyton rubrum*.

**Notes:** (A) infected skin area; (B) the fallen hair of infected area (40 $\times$ ); (C and D) *T. rubrum* colony on SDA. "a" is the hyphae growing in hair.

Ex vivo skin permeation and drug deposition studies have highlighted the crucial role of the thickening agent in determining the drug delivery characteristics of NG. The results showed  $\alpha$ NG2, formulated with a moderate Carbomer 940 proportion, exhibited a favourable balance between drug deposition and skin permeation, which is crucial for maintaining drug availability within the skin.<sup>9,19</sup> In the skin permeation study,  $\alpha$ NG2 exhibited controlled skin permeation over 24 h (Table 3), indicating an efficient release of the active ingredient without excessive systemic absorption. This result was aligned with the drug deposition findings, where  $\alpha$ NG2 demonstrated higher drug accumulation in the SC

**Table 5** The Effective and Fungal Clearance Rates at 6 d and 14 d Post-Treatment

Time	Treatments	Efficacy Rate %	Fungal Clearance Rate %
6 d post-treatment	Positive control	0	0
	$\alpha$ NG1	27.59 <sup>aA</sup>	29.17 <sup>bAB</sup>
	$\alpha$ NG2	13.79 <sup>bB</sup>	20.83 <sup>cBC</sup>
	$\alpha$ NG3	10.34 <sup>bB</sup>	12.5 <sup>dC</sup>
	TG	10.34 <sup>bB</sup>	37.5 <sup>aA</sup>
14 d post-treatment	Positive control	0	0
	$\alpha$ NG1	47.62 <sup>cC</sup>	45.83 <sup>cB</sup>
	$\alpha$ NG2	71.42 <sup>bB</sup>	79.17 <sup>bA</sup>
	$\alpha$ NG3	28.57 <sup>dD</sup>	25 <sup>dC</sup>
	TG	90.48 <sup>aA</sup>	87.5 <sup>aA</sup>

**Notes:**  $\alpha$ NG1,  $\alpha$ NG2,  $\alpha$ NG3:  $\alpha$ NE3 containing 0.5, 0.75%, and 1% (w/w) Carbomer 940; TG; within the same column, different lowercase letters indicate significant differences ( $P < 0.05$ ), and different uppercase letters indicate highly significant differences ( $P < 0.01$ ).

**Abbreviations:**  $\alpha$ NG,  $\alpha$ -pinene Nanoemulsion gel. TG, Terbinafine Hydrochloride Gel.

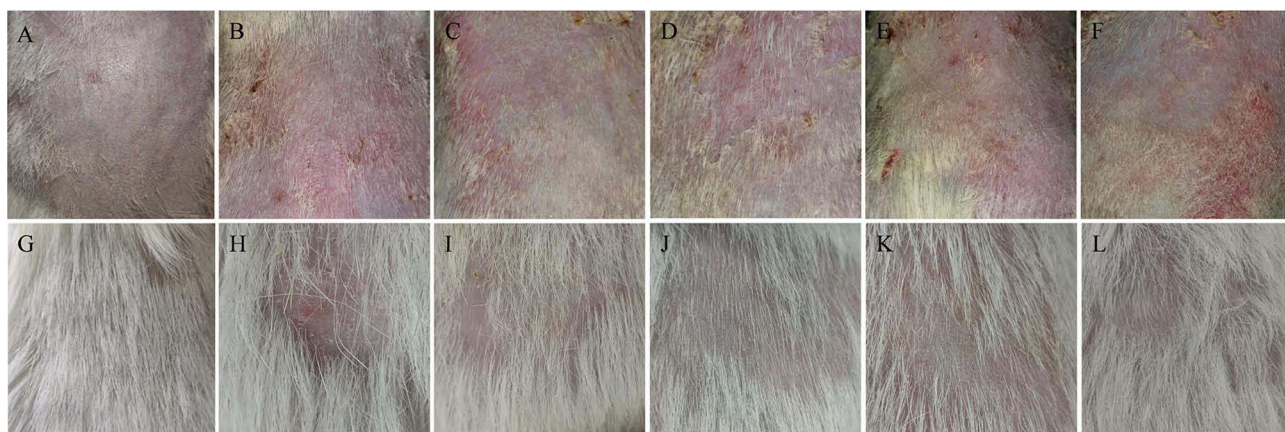


**Figure 10** The infected skin areas of different treatment groups 1 d and 14 d post-treatment.

**Notes:** (A and G) The skin area of negative control; (B and H) positive control; (C and I)  $\alpha$ NG1; (D and J)  $\alpha$ NG2; (E and K)  $\alpha$ NG3; (F and L) TG.

**Abbreviations:**  $\alpha$ NG,  $\alpha$ -piene Nanoemulsion gel; TG, Terbinafine Hydrochloride Gel.

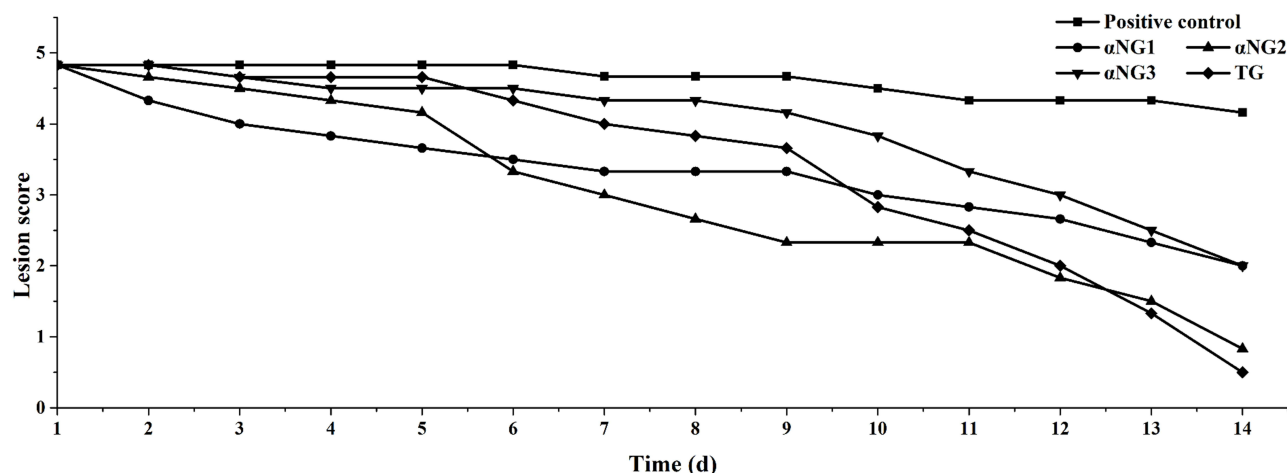


**Figure 11** The lesion scores recording in different groups during the therapeutic efficacy test.

**Abbreviations:**  $\alpha$ NG,  $\alpha$ -piene Nanoemulsion gel; TG, Terbinafine Hydrochloride Gel.

and epidermis/dermis over 12 h (Table 4), suggesting the formulation maintained effective drug concentrations at the target layers, essential for treating dermatophytosis. The balanced performance of  $\alpha$ NG2 is likely due to the gel matrix's ability to form a structured network, which effectively restricts the mobility of nanoemulsion droplets with smaller mesh sizes, thereby modulating drug release and enhancing localized drug deposition within skin layers.<sup>12,19</sup> It is worth noting that  $\alpha$ NG1's stronger skin permeation rate could also be attributed to its faster drug release rate, which allows more polysorbate 80 to interact with and potentially disrupt the integrity of SC within a given timeframe.<sup>9,13,19</sup> In contrast,  $\alpha$ NG2 and  $\alpha$ NG3, with higher Carbomer 940 proportions, showed reduced contact between polysorbate 80 and the stratum corneum, resulting in relatively weaker permeation effects.

In contrast,  $\alpha$ NG1, with a lower Carbomer 940 proportion, formed a less dense mesh network that failed to effectively restrict nanoemulsion droplet movement.<sup>9,12</sup> This led to excessive skin permeation, resulting in significant systemic absorption and insufficient drug deposition at the infection site.<sup>6,7,19,34</sup> These findings highlight the risk of insufficient drug deposition when the gel network is too loose, as the drug may be absorbed too quickly into the bloodstream before it can be deposited at the targeted skin layers. On the other hand,  $\alpha$ NG3, with a higher Carbomer 940 proportion, created an overly restrictive mesh network that limited the release and permeation of nanoemulsion droplets.<sup>9,12,19</sup> This resulted in reduced skin permeation and drug delivery efficiency, as indicated by both the skin permeation (Table 3) and drug deposition (Table 4) results. These findings highlight that  $\alpha$ NG2 optimally balances transdermal and topical drug



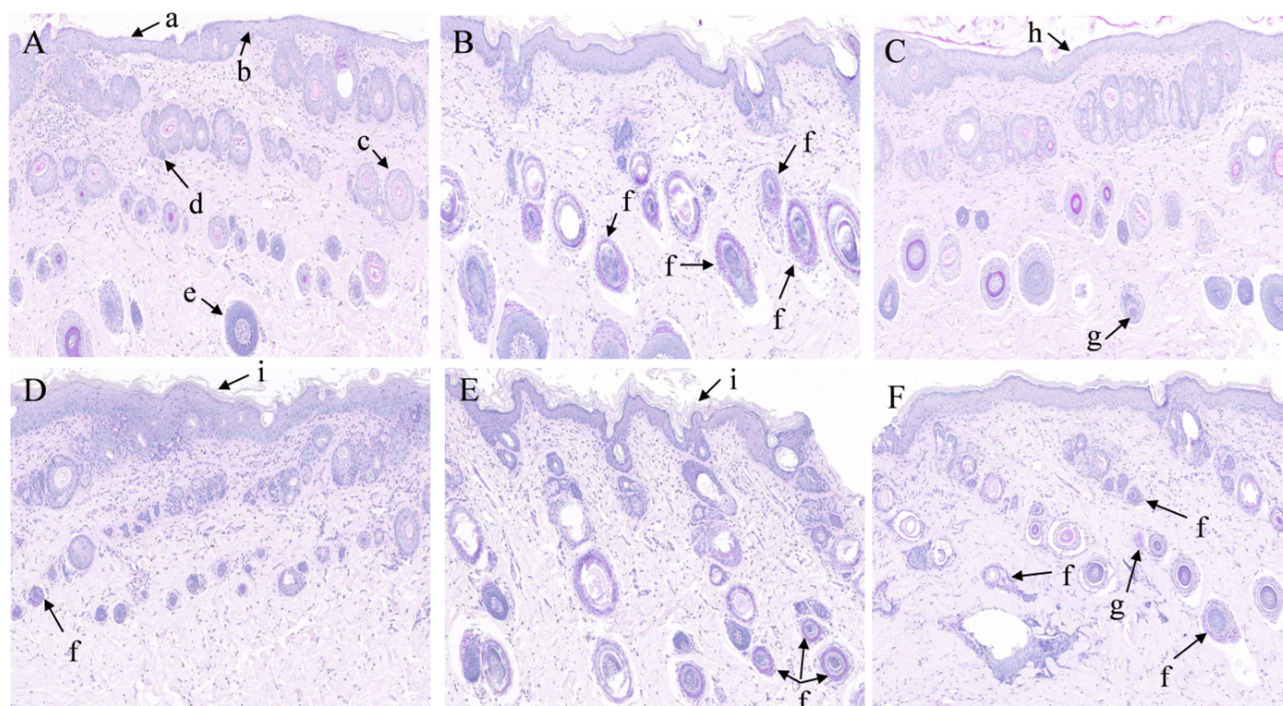


**Figure 12** The skin PAS staining section 14 d post-treatment.

**Notes:** (A) is negative control; (B) positive control; (C)  $\alpha$ NG1 group; (D)  $\alpha$ NG2; (E)  $\alpha$ NG3; (F) TG. "a" is the stratum corneum (SC); "b" epidermis; "c" hair shaft; "d" sebaceous gland; "e" hair follicle; "f" hair follicles infected by spores; "g" mycelium and spores grown in the inner root sheath; "h" the SC almost disappeared after  $\alpha$ NG1 application; "i" the relatively complete SC after  $\alpha$ NG2 or  $\alpha$ NG3 application.

**Abbreviations:**  $\alpha$ NG,  $\alpha$ -piene Nanoemulsion gel; TG, Terbinafine Hydrochloride Gel.

delivery, maintaining effective drug concentrations at the infection site. However, the less optimal Carbomer 940 proportions in  $\alpha$ NG1 and  $\alpha$ NG3 may reduce localized drug compromise their therapeutic efficacy against dermatophytosis. These suggest excessive thickening agent proportions can hinder the effective release of the drug, compromising NG's therapeutic efficacy.

These findings in skin permeation and drug deposition tests highlight the importance of optimizing thickening agent proportions to balance skin permeation and drug deposition, ensuring effective topical delivery to the infection site while avoiding systemic absorption and under-treatment.

Fluorescent imaging using coumarin-6 further confirmed the findings from skin permeation and drug deposition tests.<sup>23</sup> For  $\alpha$ NG2, fluorescence signals were predominantly localized in the epidermis/dermis (Figure 8D-F), corroborating its sustained drug levels in these layers as illustrated in the drug deposition test. This localized and controlled distribution highlights the ability of  $\alpha$ NG2 to enhance therapeutic efficacy at the infection site while minimizing systemic absorption. Conversely,  $\alpha$ NG1 exhibited pronounced fluorescence signals extending beyond the dermis (Figure 8A-C), consistent with its excessive transdermal permeation (Table 3) and rapid decline in drug deposition within the epidermis/dermis (Table 4). In the case of  $\alpha$ NG3, fluorescence was initially weak and became apparent only at 6 and 12 h (Figure 8G-I), corresponding within with reduced skin permeation and drug deposition.

It is worth noting that, in both  $\alpha$ NG2 and  $\alpha$ NG3, a bright band was observed in the SC during fluorescent imaging. This phenomenon was absent in the findings of Zheng et al,<sup>9</sup> where NG prepared with varying proportions of Carbomer 934 did not exhibit similar bright bands. The bright band in our study indicates that Carbomer 940 provides enhanced protection to SC integrity compared to Carbomer 934. This could be attributed to the denser gel network of Carbomer 940, which supports a slower and more controlled drug release,<sup>35</sup> thereby reducing potential SC disruption. This finding is consistent with our PAS staining results (arrow "i" in Figure 12D and E), which further confirm the enhanced SC protection achieved by increasing Carbomer 940 proportions. Such a mechanism contributes to the more effective drug reservoir effect,<sup>9,36</sup> ensuring localized drug availability while minimizing systemic exposure.

The use of a guinea pig model infected with *T. rubrum* in our study was instrumental in accurately simulating the dynamics of mammal dermatophyte infections, providing a reliable platform for studying their natural progression.<sup>24,25</sup> This model replicates the dermatophytic symptoms observed in other mammals, notably in keratinized structures such as the SC and hair.<sup>37</sup> By three days post-inoculation, clinical signs observed at the infection site included alopecia, scabs, white scales, and erythema. Shed skin flakes and hair were cultured on SDA plates for seven days, where microscopic examination revealed characteristic penetration of the hair shafts by fungal hyphae, with typical *T. rubrum* colonies displaying red pigment secretion. These findings validate the model's relevance for studying the infection's progression without therapeutic intervention.<sup>24,37</sup>

In the therapeutic tests,  $\alpha$ NGs demonstrated varying efficacy against *T. rubrum* infection, indicating their clinical potential.  $\alpha$ NG2 showed superior performance, maintaining effective control of infection symptoms throughout the treatment period due to its sustained-release properties as proved by drug deposition (Table 4) and fluorescent imaging (Figure 8). This consistent drug release, observed in drug deposition and skin permeation tests, prevented the resurgence of fungal growth, a common issue with other commonly used formulations.<sup>5,19</sup> mycological cultures further proved this, showing significant fungal burden reductions compared to  $\alpha$ NG1 and  $\alpha$ NG3, with similar fungal clearance rates to positive drug control TG. Conversely,  $\alpha$ NG1, with a lower Carbomer 940 proportion, allowed rapid drug penetration but quick clearance, diminishing its effectiveness.<sup>10,16</sup>  $\alpha$ NG3, with the highest Carbomer 940 proportion, restricted drug release, limiting its therapeutic potential, this was consistent with other reports, where higher thickening agent proportions render NG topical drug delivery properties rather than transdermal.<sup>9,11,34</sup> The findings highlight the critical importance of thickening agent proportions in optimizing  $\alpha$ NG2, achieving an excellent balance between skin permeation and drug deposition. This well-balanced formulation demonstrates promising clinical relevance for dermatophyte infection treatment, highlighting its potential for effective therapeutic outcomes.

Histopathological examination via PAS staining provided critical insights into skin integrity and fungal clearance post-treatment.<sup>27</sup>  $\alpha$ NG2 demonstrated the best therapeutic outcomes, eradicating fungal presence while preserving SC integrity (arrow i in Figure 12D), suggesting superior infection control with minimal skin disruption. Conversely,  $\alpha$ NG1, though effective in drug delivery (Table 3 and Figure 8A-C), disrupted the SC significantly (arrow i in Figure 12C), potentially compromising skin barrier function and increasing secondary infection risk.<sup>38</sup> Meanwhile,  $\alpha$ NG3 maintained the skin structure but failed to sufficiently reduce fungal burden, emphasizing the need to optimize the balance between drug penetration and therapeutic effectiveness to enhance treatment outcomes.

## Conclusion

In summary, our research underscores the pivotal role of thickening agent proportions in enhancing the effectiveness of nanoemulsion gels for treating dermatophytic infections. Our findings reveal that gels with varying proportions of thickening agents can produce a range of therapeutic effects. Moderate proportions, as exemplified by  $\alpha$ NG2, provide sustained drug release, combining the benefits of both transdermal and topical drug delivery. This allows for prolonged and localized action, crucial for effective dermatological treatment. Other proportions can be specifically tailored to meet distinct clinical requirements. These insights highlight the broad clinical applicability of customized nanoemulsion gels and confirm their potential as versatile treatments for various dermatological conditions.

## Funding

This study was supported by the National Natural Science Foundation of China (Grant No. 32360898), the Science and Technology Project of Guizhou Province (Grant Nos. QKHJC-ZK[2021] General 170, QKHZC [2023] General 109, and QKHPTRC-BQW[2024]007), and the Guizhou University Cultivation Project (Grant No. GDPY [2020] 82).

## Disclosure

The authors report no conflicts of interest in this work.

## References

1. Dogra S, Ramam M. Difficult Dermatophytosis. *JAMA Dermatol.* 2022;11(158):1243.
2. Bressani VO, Santi TN, Domingues-Ferreira M, Almeida A, Duarte AJS, Moraes-Vasconcelos D. Characterization of the cellular immunity in patients presenting extensive dermatophytoses due to *Trichophyton rubrum*. *Mycoses.* 2013;56(3):281–288. doi:10.1111/myc.12018
3. White TC, Findley K, Dawson TJ, et al. Fungi on the skin: dermatophytes and malassezia. *Cold Spring Harb Perspect Med.* 2014;4(8):a19802. doi:10.1101/cshperspect.a019802
4. Canete-Gibas CF, Mele J, Patterson HP, et al. Terbinafine-resistant dermatophytes and the presence of *Trichophyton indotineae* in North America. *J Clin Microbiol.* 2023;61(8):e56223.
5. Gupta AK, Ryder JE, Chow M, Cooper EA. Dermatophytosis: the management of fungal infections. *Skinmed.* 2005;4(5):305–310. doi:10.1111/j.1540-9740.2005.03435.x
6. Khurana S, Jain NK, Bedi PM. Nanoemulsion based gel for transdermal delivery of meloxicam: physico-chemical, mechanistic investigation. *Life Sci.* 2013;92(6–7):383–392. doi:10.1016/j.lfs.2013.01.005
7. Hussain A, Altamimi MA, Alshehri S, Imam SS, Shakeel F, Singh SK. Novel approach for transdermal delivery of rifampicin to induce synergistic antimycobacterial effects against cutaneous and systemic tuberculosis using a cationic nanoemulsion gel. *Int J Nanomed.* 2020;15:1073–1094. doi:10.2147/IJN.S236277
8. Kaur R, Ajitha M. Transdermal delivery of fluvastatin loaded nanoemulsion gel: preparation, characterization and in vivo anti-osteoporosis activity. *Eur J Pharm Sci.* 2019;136:104956. doi:10.1016/j.ejps.2019.104956
9. Zheng Y, Ouyang WQ, Wei YP, et al. Effects of carbopol 934 proportion on nanoemulsion gel for topical and transdermal drug delivery: a skin permeation study. *Int J Nanomed.* 2016;11:5971–5987. doi:10.2147/IJN.S119286
10. Rai VK, Mishra N, Yadav KS, Yadav NP. Nanoemulsion as pharmaceutical carrier for dermal and transdermal drug delivery: formulation development, stability issues, basic considerations and applications. *J Control Release.* 2018;270:203–225.
11. Zhang X, Wu Y, Hong Y, Zhu X, Lin L, Lin Q. Preparation and evaluation of dl-praeruptorin A microemulsion based hydrogel for dermal delivery. *Drug Deliv.* 2015;22(6):757–764. doi:10.3109/10717544.2014.898713
12. Choudhury H, Gorain B, Pandey M, et al. Recent update on nanoemulgel as topical drug delivery system. *J Pharm Sci.* 2017;106(7):1736–1751. doi:10.1016/j.xphs.2017.03.042
13. Latif MS, Nawaz A, Asmari M, Uddin J, Ullah H, Ahmad S. Formulation development and in vitro/in Vivo characterization of methotrexate-loaded nanoemulsion gel formulations for enhanced topical delivery. *Gels.* 2022;9(1):3. doi:10.3390/gels9010003
14. Varghese JS, Chellappa N, Fathima NN. Gelatin-carrageenan hydrogels: role of pore size distribution on drug delivery process. *Colloids Surf B Biointerfaces.* 2014;113:346–351. doi:10.1016/j.colsurfb.2013.08.049
15. Zhang X, Li D, Tian H, et al. Alpha-pinene is the main active ingredient of *Cacumen Platycladi* against *Trichophyton rubrum* with *ERG3* as its target. *Acta Veterinaria et Zootechnica Sinica.* 2023;Vol 54:1690–1702. in Chinese.
16. Azeem A, Rizwan M, Ahmad FJ, et al. Nanoemulsion components screening and selection: a technical note. *AAPS Pharm Sci Tech.* 2009;10(1):69–76. doi:10.1208/s12249-008-9178-x
17. Danaei M, Dehghankhold M, Ataei S, et al. Impact of particle size and polydispersity index on the clinical applications of lipidic nanocarrier systems. *Pharmaceutics.* 2018;10(2):57. doi:10.3390/pharmaceutics10020057
18. McNeil SE. *Characterization of Nanoparticles Intended for Drug Delivery.* New York: Humana Press/Springer; 2011.
19. Hussain A, Samad A, Singh SK, et al. Nanoemulsion gel-based topical delivery of an antifungal drug: in vitro activity and in vivo evaluation. *Drug Deliv.* 2016;23(2):642–647. doi:10.3109/10717544.2014.933284
20. Draize JH, Woodard G, Calvery HO. Methods for the study of irritation and toxicity of substances applied topically to the skin and mucous membranes. *J Pharmacol Exp Ther.* 1944;82(3):105–107.
21. Ng SF, Rouse JJ, Sanderson FD, Meidan V, Eccleston GM. Validation of a static Franz diffusion cell system for in vitro permeation studies. *AAPS Pharm Sci Tech.* 2010;11(3):1432–1441. doi:10.1208/s12249-010-9522-9
22. Alves MP, Scarrone AL, Santos M, Pohlmann AR, Guterres SS. Human skin penetration and distribution of nimesulide from hydrophilic gels containing nanocarriers. *Int J Pharm.* 2007;341(1–2):215–220. doi:10.1016/j.ijpharm.2007.03.031
23. Finke JH, Richter C, Gothsch T, Kwade A, Büttgenbach S, Goymann CCM. Coumarin 6 as a fluorescent model drug: how to identify properties of lipid colloidal drug delivery systems via fluorescence spectroscopy? *Eur J Lipid Sci Technol.* 2014;116(9):1234–1246. doi:10.1002/ejlt.201300413
24. Chen XJ, Shen YN, Lü G, Liu WD. Establishing an experimental Guinea pig model of dermatophytosis using *trichophyton rubrum*. *Acta Academiae Medicinae Sinicae.* 2008;30(5):599–602. in Chinese.
25. Garvey EP, Hoekstra WJ, Moore WR, Schotzinger RJ, Long L, Ghannoum MA. VT-1161 dosed once daily or once weekly exhibits potent efficacy in treatment of dermatophytosis in a guinea pig model. *Antimicrob Agents Chemother.* 2015;59(4):1992–1997. doi:10.1128/AAC.04902-14
26. Sajitha K, Carol FZ. Efficacy of antifungal treatment in the clinicomycological cure of *T. Corporis/T. Cruris* *J Evol Med Dent Sci.* 2017;6(66):4765–4768. doi:10.14260/Jemds/2017/1032
27. Shalin SC, Ferringer T, Cassarino DS. PAS and GMS utility in dermatopathology: review of the current medical literature. *J Cutan Pathol.* 2020;47(11):1096–1102. doi:10.1111/cup.13769
28. Bhattacharjee S. DLS and zeta potential - what they are and what they are not? *J Control Release.* 2016;235:337–351. doi:10.1016/j.jconrel.2016.06.017
29. Clogston JD, Patri AK. Zeta potential measurement. *Methods mol Biol.* 2011;697:63–70.
30. Erramreddy VV, Ghosh S. Influence of emulsifier concentration on nanoemulsion gelation. *Langmuir.* 2014;30(37):11062–11074. doi:10.1021/la502733v
31. Al-Hussaniy H, Almajidi Y, Oraibi A, Alkarawi A. Nanoemulsions as medicinal components in insoluble medicines. *Farmatsiia.* 2023;3(70):537–547.
32. Ojha B, Jain VK, Gupta S, Talegaonkar S, Jain K. Nanoemulgel: a promising novel formulation for treatment of skin ailments. *Polym Bull.* 2021;79(42):4441–4465.
33. Ma Q, Zhang J, Lu B, et al. Nanoemulgel for improved topical delivery of desonide: formulation design and characterization. *AAPS Pharm Sci Tech.* 2021;22(5):163. doi:10.1208/s12249-021-02035-5

34. Kaur A, Katiyar SS, Kushwah V, Jain S. Nanoemulsion loaded gel for topical co-delivery of clobetasol propionate and calcipotriol in psoriasis. *Nanomedicine*. 2017;13(4):1473–1482. doi:10.1016/j.nano.2017.02.009
35. Unlü N, Ludwig A, Ooteghem MV, Hincal AA. A comparative rheological study on carbopol viscous solutions and, the evaluation of their suitability as the ophthalmic vehicles and artificial tears. *Pharm Acta Helv*. 1992;67(1):5–10.
36. Hafeez F, Chiang A, Hui X, Zhu H, Kamili F, Maibach HI. Stratum corneum reservoir as a predictive method for in vitro percutaneous absorption. *J Appl Toxicol*. 2016;36(8):1003–1010. doi:10.1002/jat.3262
37. Saunte DM, Hasselby JP, Brillowska-Dabrowska A, et al. Experimental Guinea pig model of dermatophytosis: a simple and useful tool for the evaluation of new diagnostics and antifungals. *Med Mycol*. 2008;46(4):303–313. doi:10.1080/13693780801891732
38. Del RJ, Levin J. The clinical relevance of maintaining the functional integrity of the stratum corneum in both healthy and disease-affected skin. *J Clin Aesthet Dermatol*. 2011;4(9):22–42.

International Journal of Nanomedicine

Publish your work in this journal

The International Journal of Nanomedicine is an international, peer-reviewed journal focusing on the application of nanotechnology in diagnostics, therapeutics, and drug delivery systems throughout the biomedical field. This journal is indexed on PubMed Central, MedLine, CAS, SciSearch®, Current Contents®/Clinical Medicine, Journal Citation Reports/Science Edition, EMBase, Scopus and the Elsevier Bibliographic databases. The manuscript management system is completely online and includes a very quick and fair peer-review system, which is all easy to use. Visit <http://www.dovepress.com/testimonials.php> to read real quotes from published authors.

Submit your manuscript here: <https://www.dovepress.com/international-journal-of-nanomedicine-journal>

**Dovepress**  
Taylor & Francis Group